



HHS Public Access

Author manuscript

J Med Chem. Author manuscript; available in PMC 2018 July 13.

Published in final edited form as:

J Med Chem. 2017 July 13; 60(13): 5507–5520. doi:10.1021/acs.jmedchem.7b00189.

Structure-Based Optimization of Pyridoxal 5'-Phosphate-Dependent Transaminase Enzyme (BioA) Inhibitors that Target Biotin Biosynthesis in *Mycobacterium tuberculosis*

Feng Liu[†], Surendra Dawadi[†], Kimberly M. Maize[†], Ran Dai[†], Sae Woong Park[‡], Dirk Schnappinger[‡], Barry C. Finzel^{*,†}, and Courtney C. Aldrich^{*,†}

[†]Department of Medicinal Chemistry, University of Minnesota, Minneapolis, Minnesota 55455, United States

[‡]Department of Microbiology and Immunology, Weill Cornell Medical College, New York, New York 10065, United States

Abstract

The pyridoxal 5'-phosphate (PLP)-dependent transaminase BioA catalyzes the second step in the biosynthesis of biotin in *Mycobacterium tuberculosis* (*Mtb*) and is an essential enzyme for bacterial survival and persistence in vivo. A promising BioA inhibitor **6** containing an *N*-aryl, *N'*-benzoylpiperazine scaffold was previously identified by target-based whole-cell screening. Here, we explore the structure–activity relationships (SAR) through the design, synthesis, and biological evaluation of a systematic series of analogues of the original hit using a structure-based drug design strategy, which was enabled by cocrystallization of several analogues with BioA. To confirm target engagement and discern analogues with off-target activity, each compound was evaluated against wild-type (WT) *Mtb* in biotin-free and -containing medium as well as BioA under- and overexpressing *Mtb* strains. Conformationally constrained derivative **36** emerged as the most potent analogue with a K_D of 76 nM against BioA and a minimum inhibitory concentration of 1.7 μ M (0.6 μ g/mL) against *Mtb* in biotin-free medium.

Graphical abstract

^{*}Corresponding Authors: Phone: 612-626-5979. Fax: 612-626-3114. finze007@umn.edu.; Phone: 612-625-7956. Fax: 612-626-3114. aldri015@umn.edu.

Supporting Information

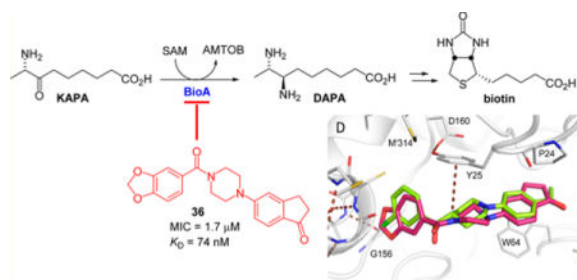
The Supporting Information is available free of charge on the ACS Publications website at DOI: 10.1021/acs.jmedchem.7b00189. X-ray crystallographic data and copies of ¹H and ¹³C NMR spectra (PDF) Molecular formula strings (CSV)

ORCID

Courtney C. Aldrich: 0000-0001-9261-594X

Notes

The authors declare no competing financial interest.



INTRODUCTION

Tuberculosis (TB) is both an ancient scourge and a current global health crisis.¹ The common ancestor of *Mycobacterium tuberculosis* (*Mtb*) and other members of the *Mtb* complex is thought to have evolved in Africa approximately 70,000 years ago,² and evidence of *Mtb* infection has been found in New Kingdom Egyptian³ as well as pre-Columbian Peruvian⁴ mummies. Today, TB is one of the top 10 causes of death worldwide.⁵ In 2015, there were approximately 1.8 million deaths from TB, including 400,000 deaths of those also infected with HIV according to the World Health Organization (WHO).⁵ On the basis of the Joint United Nations Programme on HIV/AIDS (UNAIDS) reports, TB is the leading cause of death in HIV-positive populations,⁶ accounting for more than 35% of all deaths from AIDS-associated diseases.^{5,6} Although the worldwide prevalence of TB is decreasing, it remains a threat, particularly to the HIV-positive population.⁷

The current first-line therapy recommendation is for 2 months of HRZE (isoniazid, rifampicin, pyrazinamide, and ethambutol, respectively) followed by a 4 month continuation of HR therapy.⁸ Although treatment-resistant TB has existed since the introduction of modern TB therapeutics,⁹ drug-resistant TB has now emerged as a global challenge, making the standard drugs isoniazid and rifampicin ineffective toward combating some cases of *Mtb*.¹⁰ The World Health Organization estimates that nearly half a million new cases of multidrug resistant tuberculosis (MDR-TB) will occur each year.¹¹ MDR-TB is particularly prevalent in China, India, and Russia; these three countries account for more than 50% of all MDR-TB cases.¹⁰ Moreover, extensively drug-resistant TB (XDR-TB) is more challenging to treat, resulting in an extremely high mortality rate. On its own, XDR-TB is a burgeoning major global health problem.^{12,13} Treatment success rates for TB, MDR-TB, and XDR-TB are 83, 52, and 28%, respectively.⁵ Control of the TB epidemic is further complicated by latent infections, and it is estimated that one in three people worldwide are infected with *Mtb*.^{14,15} Consequently, there is an urgent need to develop drugs that act on novel targets.^{14,16–20}

One approach to designing new TB therapies is to target metabolic processes essential in both active and latent stages of *Mtb*. Biotin (vitamin H, vitamin B₇) biosynthesis is one such pathway.²¹ Biotin **5** (Scheme 1) is an essential cofactor utilized by carboxylases in fatty acid metabolism and gluconeogenesis pathways.²² Humans obtain biotin from intestinal microflora, dietary sources, and recycling.²³ However, *Mtb* synthesizes biotin de novo²⁴ because it cannot obtain sufficient levels of biotin to support growth in either mouse or

man,²⁸ which makes the biotin biosynthesis pathway an attractive target for new drug discovery.

Biotin biosynthesis in *Mtb* involves the conversion of pimeloyl-CoA **1** to biotin **5** (Scheme 1) using the reactions catalyzed by enzymes 7-keto-8-aminopelargonic acid (KAPA) synthase BioF, 7,8-diaminopelargonic acid (DAPA) synthase BioA, dethiobiotin (DTB) synthetase (BioD), and biotin synthase (BioB). BioA, the target enzyme of the present work, is the second enzyme in this pathway. A pyridoxal 5'-phosphate (PLP)-dependent enzyme, BioA catalyzes the transamination of KAPA **2** to DAPA **3** using *S*-adenosylmethionine (SAM) as an amino donor.^{25–27} BioA has been shown to be essential for bacterial persistence in a murine model of TB, making it a promising target for novel TB therapy.²⁸ BioA has been structurally characterized²⁹ and is amenable to biochemical characterization.²⁷ As such, it has been a target of our drug discovery efforts, and we have identified several small molecule inhibitors of BioA, including reversible covalently modifying hydrazines,³⁰ an irreversible covalent inhibitor developed from amiclennomycin^{31–33} and compounds identified through conventional in vitro screening approaches.³⁴

Most recently, a number of potent hits have been identified by a target-based whole-cell screening approach including *N*-aryl, *N'*-benzoylpiperazine **6**, which was identified as the most promising hit based on its combination of potency and selectivity (Figure 1A).³⁵ The compound shows good inhibition of BioA with an IC₅₀ of 155 nM and reasonable on-target activity against whole-cell *Mtb* in biotin-free medium with a minimum inhibitor concentration of 26 μM and no observed activity in biotin-supplemented medium.^{35,36} It has a structural core comprised of a piperazine ring flanked by two aryl groups each attached to a piperazine nitrogen: a 4-acetylphenyl ring on one side and a methylene-3,4-dioxybenzoyl group on the other. To guide the structure-based optimization of **6**, we cocrystallized **6** in complex with BioA and subsequently solved the X-ray crystal structure at 1.6 Å resolution (Table S1; PDB ID: 4XJP).³⁶ The complex shows that inhibitor **6** extends across the length of a partially induced binding groove at the BioA monomer–monomer interface and atop the PLP cofactor. However, comparison of the shape of the BioA pocket to the shape of the ligand in the complex led us to believe that opportunities for further inhibitor optimization exist.

Guided by molecular structures, we have prepared three series of analogues of **6** to explore the structure–activity relationship (SAR) of this scaffold (Figure 1B). The first series investigated the replacement of the benzodioxole group with a number of aromatic systems, a process that we call P1 (pocket 1) optimization. The second series explored modification of the 4-acetylphenyl ring with various aromatic systems while keeping the best aryl moiety at the P1 optimization site, which we call P2 optimization. The third series replaced the central piperazine core with other isosteres. Combining some of the best features from these series has led to the discovery of inhibitors more potent than the original hits.

RESULTS AND DISCUSSION

Structure–Activity Relationship (SAR) Studies

Assessment of the antitubercular activity of all compounds was performed using the protocol described by Park et al.³⁵ The minimum inhibitory concentrations (MICs) were determined with wild-type (WT) *Mtb* H37Rv in biotin-free and -containing medium to identify compounds with biotin-dependent activity. To provide further support for the mechanism of action, we also evaluated the activity of every compound against BioA under- and overexpressing *Mtb* strains (BioA-UE and BioA-OE, respectively). BioA-UE expresses approximately 20% of BioA relative to WT *Mtb* and is therefore more sensitive to BioA inhibitors, whereas BioA-OE expresses approximately 1200% of BioA relative to WT *Mtb* and thus should be more resistant to BioA inhibitors.

P1 Optimization—The benzodioxole group of **6** binds into a pocket (P1) at one end of the ligand binding groove. Unlike P2, which is in part comprised of conformationally malleable amino acid side chains, P1 is lined largely by backbone atoms that appear to be more rigid (Figure 2A). In P1, the benzodioxole group is bound by Gly156-Tyr157 and a helical turn formed by residues Cys168-Gly172, and it stacks directly alongside the peptide joining Gly172 to Gly173. Most of the protein heteroatoms lining this pocket are already engaged in hydrogen bonding with other protein atoms. Gly156 O, for example, is H-bonded to Asp169 NH. Consequently, the subsite is polar, but it does not afford many opportunities for additional H-bonding. Such a site is well-suited to accommodate the benzodioxole moiety of **6**.

There is, however, poor shape complementarity between the benzodioxole group and the pocket surrounding it, suggesting that better substituents to fill this pocket might be found. A series of alternatives to the benzodioxole group were explored (Table 1). It seemed that the 1,3-benzodioxole moiety of **6** was inadequate to completely fill the subsite, so larger benzodioxoles, i.e., 1,4-benzodioxole **7** and 1,5-benzodioxole **8**, were explored. The dimension of the P1 pocket was further tested with smaller 5-membered heterocycles **15** and **16**. All of these modifications drastically reduced potency under all conditions. In retrospect, the larger aliphatic bridges of compounds **7** and **8** likely cannot be accommodated alongside the Gly172 peptide bond as in **6**. If the ring were to flip 180° around the aryl-amide bond, a steric clash would arise with Tyr25.

On the other hand, the 3,4-dichlorophenyl analogue **9**, which is a close conformational mimic of the 1,3-benzodioxole moiety, was reasonably well-tolerated with a 2-fold loss in potency against WT *Mtb* in biotin-free medium. The findings that this compound had equal susceptibility against WT *Mtb* in biotin-containing medium indicates undesirable off-target activity. Removing the 4-chloro group produced the 3-chlorophenyl analogue **12**, which showed slightly improved activity against WT *Mtb* over the original hit **6** and, unlike **9**, maintained on-target activity as judged by its activity profile. Comparison of the crystal structure of the complex of BioA and **12** (PDB ID: 4W1X) with **6** (PDB ID: 4XJP) shows that these two compounds bind very similarly.^{35,36}

There also appeared to be a penetrable gap between Tyr25 and Cys168 that might be filled with substituents extending from the 5-position of the 3-chlorophenyl ring. This led to the synthesis of analogues **10** and **11** but neither produced improvements in potency over **6**. One explanation for the inactivity of select compounds **10** and **11** may be that any atom directly connected to the 5-position of the chlorobenzene ring must pass very close to the OH of Tyr25, which is already donating the hydrogen to Asp160 and might therefore repel the large chlorine (**10**) or electronegative oxygen (**11**). Replacement of the phenyl ring with a pyridyl ring in chloropyridyl **13** and pyridyl **14** obliterated activity, which together with the lack of activity of the aforementioned thiazole **15** and pyrazole **16** derivatives demonstrates that the presence of a phenyl ring at the P1 position is highly favorable. To complete our exploration of the P1 subsite, we prepared a series of aliphatic analogues (**17–20**) that were devoid of activity except for **19**, which was nearly equipotent to **6** against WT *Mtb*. However, the MIC of **19** was insensitive to exogenous biotin or BioA underexpression suggesting the activity of this compound is largely due to off-target effects.

P2 Optimization—Compounds **6** and **12** share a common orientation for the 4-acetylphenyl group in a hydrophobic pocket (P2) bound by the side chains of Pro24 and Trp64 and loops Met⁹¹-Gly⁹³ and Pro³¹⁷-Thr³¹⁸ (Figure 2A). (Here, and throughout this discussion, a prime in the residue number identifies residues in the alternate monomer of the BioA homodimer). Trp64 is induced into a side chain conformation that enables π - π stacking extending across the length of the acetylphenyl group, affirming the importance of an aromatic substituent in P2. The acetyl carbonyl oxygen accepts a hydrogen bond from the backbone amide of Gly⁹³, but backbone carbonyl groups from residues Pro³¹⁷ and Thr³¹⁸ that are directed into the subsite make only weakly stabilizing polar interactions with the acetyl methyl group (e.g., C-H...O hydrogen bonds). The next priority in exploring analogue SAR was to modify the acetylphenyl group of **12** to explore more diverse functional groups (Table 2).

The dimensions of P2 were tested with biphenyl moieties (e.g., **21** and **22**) that are privileged structures in drug discovery³⁷ as well as smaller heterocyclic biphenyls (**23–25**). Of the compounds bearing a biphenyl-like group, only oxazole **25** was as effective as the original hit. Most other functional group substitutions at the 4-position of the phenyl ring were inactive. The introduction of a methyl group in **23** and **24** obliterated activity. The loss of activity by several of these can be attributed in retrospect to the apparent inflexibility of the backbone of residues ³¹⁷-³¹⁸, which, left unmoved, forms a stout wall of H-bond acceptors inside the pocket that must resist interactions with H-bond acceptors of **31–33**. The position of the acetyl group is critical; *meta*-acetyl analogue **30** lost nearly 10–50-fold in activity compared to the *para*-acetyl **12** against WT *Mtb* and Bio-UE *Mtb* strains. The thiophene of **34** likely serves as a respectable isostere of **12** and retains comparable (but not superior) activity. The replacement of the keto group with a ketoxime group of **35** resulted in inferior activity. Several 3,4-bicyclic analogues (**26–29**) were inspired by the overlay of the acetylphenyl group of **6** or **12** with an inden-1-one moiety found and characterized in fragment screening (Figure 2B,C).³⁸ These compounds generally retained some biological activity, but only compound **26** with the identical inden-1-one of the original fragment hit improved upon the activity of **12**. A crystal structure of the complex with **26** (Table S1; PDB

ID: 4XJO³⁶) was determined. This structure confirms the predicted binding mode and affirms the position of the inden-1-one with an H-bond to Gly'93 NH (2.8 Å) as well as tight packing against carbonyl oxygen atoms of Pro'317 and Thr'318 by carbon atoms in the five-membered carbocycle (3.5 and 3.6 Å, respectively).

Central Core Exploration—Several heterocyclic alternatives to the piperazinyl carbonyl linker in the central core were explored (Table 3). Smaller inflexible triazole linkers (**37** and **38**) were inactive. Interestingly, the corresponding piperidinyl analogues of **12** and **6** (**39** and **40**, respectively) showed divergent activity. The chlorophenyl analogue **39** delivered modest antitubercular activity, although much of that activity may be off-target. The benzodioxole analogue **40** was completely inactive. We obtained a crystal structure of the complex with **39** (Table S1, Figure 2D, PDB ID: 5KGT). Both **6** and **12** derive some potency from planar stacking between the amide bond of the piperazinyl carbonyl and Tyr25.³⁸ The amide plane is absent in piperidinyl analogues, but in the complex with **39**, the ring pucker permits a perfectly positioned C–H on C4 of the piperidine to donate a H-bond to the Tyr25 π -system, whereas the position of the chlorophenyl ring is consistent with the positioning of the same moiety in the complex with **12**. To rationalize the complete lack of activity for **40**, the analogous crystal structure of **6** was examined. This structure shows that the piperazine in **6** must twist significantly to accommodate the benzodioxole in P1; a comparable twist applied to the piperidine of **40** likely forces C4 out of proper alignment for a good interaction with Tyr25, resulting in lower affinity and inactivity.

Combining the best of the P1 substituents with the best P2 group and flexible piperazinyl linker resulted in compound **36**, which has potent antitubercular activity with an improved MIC of 1.7 μ M against WT *Mtb* in biotin-free medium (Table 3). Moreover, **36** displays biotin and BioA-dependent activity, consistent with the desired mechanism of action (Table 3 and Figure 3). We obtained the crystal structure of BioA with **36** (Table S1, Figure 2D, PDB ID: 5KGS), which showed conserved binding modes for each of its distinct substituents. The binding mode of the inden-1-one P2 substituent is highly similar to that of **26** in structure 4XJO³⁶ (Table S1). A slight difference in planar orientation can be attributed to a twist in the piperazinyl carbonyl core that appears to coincide with the P1 substituent identity; one position is observed with the benzodioxole P1 group (**6**, **36**), whereas the other position is observed in compounds with 3-chlorophenyl P1 groups (**12** and **26**). To yield the conserved piperazinyl carbonyl core twist, the benzodioxole group of **36** is bound in the same fashion as the benzodioxole group of **6**.

Overall, the SAR studies have shown that compounds **6**, **12**, **25–28**, and **36** are effective inhibitors of both BioA and *Mtb* with MIC values from 1.7 (**36**) to 35 μ M (**27**). Other compounds (**9**, **11**, **19**, **22**, and **32–35**) inhibit WT *Mtb* with MIC values from 9.9 (**34**) to 40.8 μ M (**29**), but these compounds do not show biotin-dependent activity nor the predicted monotonic behavior with BioA expression levels from the BioA-UE, BioA-OE, WT-biotin, and WT+biotin inhibition experiments.

Binding Affinity by Isothermal Titration Calorimetry (ITC)

BioA binding affinity (K_D) and thermodynamic parameters (ΔH , ΔS) of selected compounds were determined by isothermal titration calorimetry (ITC) as shown in Table 4 with representative ITC data illustrated in Figure 4. The K_D values correlate well with the corresponding MIC values. The most potent compound, **36**, possessed a BioA K_D value of 74 nM. The tested compounds have a range of potencies spanning approximately 1 order of magnitude from 74 to (**36**) to 886 nM (**28**).

Changes in the P1 group produce a consistent energetic profile. Compounds incorporating the benzodioxole (compounds **6** or **36**) reflect a significant enthalpic benefit upon binding but at moderate entropic cost. This is a pattern expected to be found when good specific interactions that restrict binding conformation are made. In the case of the benzoxazole, the excellent geometry of weak CH \cdots O interactions with Gly156 O and Cys168 C β H, and Gly227 C α H can explain this stabilization pattern. Compounds that incorporate the chlorophenyl in P1 consistently show a more balanced contribution to binding that are favorable in both enthalpy and entropy. The chlorine of **12** lies centered between these same protein structural elements but does not impose the same directional restraints as C \cdots H interactions made by the methylene bridge of the dioxolane.

We anticipated that cyclizing the acetylphenyl P2 group of **6** or **12** (resulting in **36** or **26**, respectively) might result in a smaller entropic binding penalty, but no consistent trend confirming this prediction emerges from the ITC data. Alternate P2 closed-ring systems (**27** and **28**) were also explored using ITC. However, neither of these compounds were especially potent or had significantly different thermodynamic parameters (Table 4).

In addition to potency, the thermodynamic parameters of binding can be key elements in determining the best clinical candidate. Enthalpy-driven hits are often preferred because they may be more amenable to future optimization.^{39–41} In our series, the most potent inhibitor (**36**) is driven by enthalpic stabilization but has an entropic binding cost, which may provide an opportunity for future improvement.

Synthetic Chemistry

For the preparation of inhibitors in the P1 optimization series that involved modification of the 1,3-benzodioxole ring with various other aromatic systems, the synthesis started from condensation of piperazine **41** with 4'-fluoroacetophenone to afford monoaroylated intermediate **42** (Scheme 2). Subsequent coupling with various carboxylic acids using standard EDC-mediated conditions provided compounds **6–11** and **13–20**. Similarly, compound **36** was synthesized by the condensation of **41** with 5-fluoro-1-indanone to furnish intermediate **43**, which after EDC coupling with piperonylic acid afforded **36** (Scheme 2).

The synthesis of inhibitors in the P2 optimization series with modification of the acetylphenyl ring started with monoaroylation of piperazine **41** with 3-chlorobenzoyl chloride generated *N*-(3-chlorobenzoyl)piperazine **44** using a previously reported procedure (Scheme 3).⁴² Palladium-catalyzed amination⁴³ in the presence of Cs₂CO₃ with an aryl

bromide afforded compounds **12**, **21–24**, and **26–34**. However, preparation of the remaining two compounds in the series involved the functional group interconversions of methyl ketone **12** to isoxazole **25** and oxime **35**. Condensation of **12** with *N,N*-dimethylformamide dimethyl acetal in *o*-xylene provided the keto-enamine intermediate, which when treated with hydroxylamine hydrochloride in EtOH, underwent subsequent condensation to afford **25** (Scheme 3). Ketoxime **35** was prepared by the reaction of ketone **12** with hydroxylamine hydrochloride in EtOH.

For linker optimization, two different linker moieties were employed for the replacement of piperazine, 1,2,3-triazoles, and piperidine. Synthesis of inhibitors with the 1,2,3-triazoles linker began with substitution of 3-chlorobenzyl chloride **45** with sodium azide to provide intermediate **46**.⁴⁴ Subjection of azide **46** and the corresponding terminal alkynes to standard click chemistry conditions afforded **37** and **38** (Scheme 4). For the synthesis of inhibitors with a piperidine linker, the amino group of isonipecotic acid **47** was Boc protected followed by the conversion of the carboxylic acid to Weinreb amide **48** (Scheme 5).⁴⁵ Addition of an aryllithium species to **48** afforded compounds **49** and **50**. Deprotection of the Boc group with TFA followed by palladium-catalyzed amination with 4-bromoacetophenone furnished analogues **39** and **40**.

CONCLUSIONS

The SAR of *N*-aryl, *N'*-benzoylpiperazine **6**³⁵ was explored through the preparation of 34 analogues that comprehensively examined the P1 group, P2 group, and piperazinyl carbonyl core. The synthetic modifications were informed by multiple cocrystal structures of analogues in the series. After investigating smaller and larger cyclic groups as well as aliphatic groups, the best P1 groups were found to be benzodioxole and 3-chlorophenyl. In the P2 group, only modification to an inden-1-one group resulted in analogues with increased antitubercular activity. Explorations of the central core led to the conclusion that the piperazinyl carbonyl core geometry is necessary for optimal P1 group binding. Although many of the analogues displayed the expected BioA and biotin-dependent whole-cell activity, we also observed several compounds that did not and therefore act through alternate mechanisms, which helped clarify interpretation of the SAR. For example, compound **19** containing a pentyl side chain at P1 and compound **32** with a 4-cyanophenyl group at P2 each displayed nearly equal activity in biotin-free and -containing media. Moreover, the activity did not vary significantly with BioA expression levels. Given the relatively simple nature of the initial *N*-aryl, *N'*-benzoylpiperazine scaffold, it is not altogether surprising that some analogues could engage alternate targets because *N*-arylpiperazines have many reported bioactivities. However, our analysis rapidly identified these off-targets hits and allowed us to remain focused on compounds that operate through the desired mechanism of action. Compound **26** containing the optimal P1 and P2 groups maintained the excellent bioactivity of the initial hit, but successfully removed the methylenedioxy group, a known toxicophore, and one rotatable bond through cyclization of the methyl ketone back onto the phenyl ring. Compound **36** emerged as the most potent analogue with a minimum inhibitory concentration of 1.7 μ M against *Mtb* in biotin-free medium. Structures of BioA with both **26** and **36** indicate that the binding modes are nearly identical to **6**, and thermodynamic data

show that the binding is strongly enthalpy driven. Optimization of the thermodynamic parameters of compounds like **36** to achieve additional entropic stabilization may present a future avenue for the development of even more potent BioA inhibitors.

EXPERIMENTAL SECTION

BioA Protein Expression and Purification

N-terminally His-tagged BioA was overexpressed in *Escherichia coli* and purified using Ni affinity and size exclusion chromatography as described previously.^{34,46} Full saturation of the active site by the PLP cofactor was ensured by adding 1 mM PLP to pooled protein as eluted from the SEC column and confirmed using differential scanning fluorimetry as previously described.^{34,46}

Crystallography

Crystals of BioA were obtained by hanging drop vapor diffusion at 20 °C and a microseeding technique under conditions of 100 mM HEPES pH 7.5 (Sigma Life Science), 100 mM MgCl₂ (EMD Chemicals), and 10–14% PEG 8000 (Acros Organics); drops consisted of 2 μL of protein solution (13 mg/mL) in buffer from purification, 1.5 μL of well solution, and 0.5 μL of seed solution as previously reported.^{30,35,38} Complexes were obtained by soaking using a 5 mM final concentration of the ligand. Co-crystals may also be obtained using the drop setup as above supplemented with 0.15 μL of ligand solution (50 mM). Crystals were cryoprotected using well solution supplemented with 15% PEG 400 (Sigma Life Science), followed by flash vitrification in liquid nitrogen.

Data for structures 4XJO, 4XJP, and 5KGS were collected at APS beamline 17-ID (IMCA-CAT) equipped with a Dectris Pilatus 6 M detector at 100 K. Data for structure 5KGT were collected at ALS beamline 4.2.2 equipped with an RDI 8 M detector at 100 K. The data were processed using AutoProc⁴⁷ or XDS⁴⁸ and solved with Phaser,⁴⁹ using the coordinates from structure 4W1X or 3TFT.^{31,35} Refinement was carried out in Phenix,^{50,51} and visualization was performed in Coot.⁵² Ligand restraints were calculated using JLigand.⁵³

Isothermal Titration Calorimetry (ITC)

ITC was conducted on a MicroCal Auto-iTC200 microcalorimeter (Malvern Instruments Ltd., UK) with a cell volume of 200 μL and a syringe volume of 40 μL . All experiments were performed at 25 °C in ITC buffer (25 mM HEPES [pH 7.5] and 50 mM NaCl). BioA was exchanged into this buffer using an Amicon Ultra concentrator, and the final enzyme concentration was determined using a NanoDrop instrument with the calculated extinction coefficient ϵ_{280} ($\epsilon_{280} = 64900 \text{ M}^{-1} \text{ cm}^{-1}$). The concentration of BioA was 10 μM . The ligand concentration was 100 μM , which was prepared by diluting a 20 mM DMSO stock with the ITC buffer. DMSO was added to the corresponding BioA protein solution to equalize the DMSO concentrations. All titrations were performed with a stirring speed of 750 rpm and a 150 s interval between 2 μL injections. The initial injection was not used for data fitting. Titrations were run past the point of enzyme saturation to determine and correct the heats of dilution. Data were fit to a theoretical titration curve using the Origin software package (version 7.0) provided with the instrument to obtain K_A (the association constant in

M^{-1}) and H (enthalpy) of binding. The thermodynamic parameters (G and $-T S$) are calculated using eq 1

$$\Delta G = -RT \ln K_A = \Delta H - T \Delta S \quad (1)$$

where G , H , and S are the changes in free energy, enthalpy, and entropy of binding, respectively, $R = 1.98 \text{ cal mol}^{-1} \text{ K}^{-1}$, and T is the absolute temperature. The affinity of the ligands for BioA is provided as the dissociation constant ($K_D = 1/K_A$). Average thermodynamic parameters and standard errors (Table 4) were computed from triplicate experiments.

***Mtb* Whole-Cell Growth Assay (MIC Determination)**

The *Mtb* whole-cell assay for the MIC determination was performed using a method previously described.³⁵ Briefly, *Mtb* WT, BioA-UE, and BioA-OE were grown in Sauton's medium (0.5 g KH_2PO_4 , 0.5 g of $\text{MgSO}_4 \cdot 7\text{H}_2\text{O}$, 2.0 g of citric acid, 0.05 g of ferric ammonium citrate, 60 mL of glycerol, 4.0 g of asparagine, 0.1 mL of 1% ZnSO_4 , and 0.02% tyloxapol in 1 L) containing 1 μM biotin to an $\text{OD}_{580 \text{ nm}}$ between 1.0 and 1.2. The cells were subsequently harvested by centrifugation, washed twice with biotin-free Sauton's medium, and diluted in 96-well plates to an $\text{OD}_{580 \text{ nm}}$ of 0.03. To set up the *Mtb* WT with or without biotin plates, 1 μM biotin or no biotin was added to the plates, respectively. To set up the *Mtb* BioA-UE or BioA-OE plates, 200 ng/mL anhydrotetracycline was added to the plates containing BioA-UE or BioA-OE stain, respectively, to achieve the desired level of BioA expression.

The compounds were added to final concentrations between 0.2 and 50 μM . Wells containing no compound were used as controls. Plates were incubated at 37 °C, and optical density was measured after 9 days. All growth assays were performed in triplicate with two biological replicates. MIC values were calculated using Prism (version 5.01).

Synthesis

General—Chemicals and solvents were purchased from Acros Organics, Alfa Aesar, Sigma-Aldrich, and TCI America and were used as received. An anhydrous solvent dispensing system using two packed columns of neutral alumina was used for drying THF and CH_2Cl_2 , and the solvents were dispensed under argon gas (Ar). EtOAc and hexanes were purchased from Fisher Scientific. TLC analyses were performed on TLC silica gel plates 60 F₂₅₄ from EMD Millipore Inc. and were visualized with UV light. Purification by flash chromatography was performed using a medium-pressure flash chromatography system equipped with flash column silica cartridges with the indicated solvent system. ^1H and ^{13}C spectra were recorded on a 400 MHz Varian NMR spectrometer. Proton chemical shifts are reported in ppm from an internal standard of residual chloroform (7.26), methanol (3.31), dimethyl sulfoxide (2.50), or monodeuterated water (HDO, 4.79); carbon chemical shifts are reported in ppm from an internal standard of residual chloroform (77.2), methanol (49.1), or dimethyl sulfoxide (39.5). Proton chemical data are reported as follows: chemical shift, multiplicity (s = singlet, d = doublet, dt = doublet of triplets, t = triplet, q = quartet,

pent = pentet, m = multiplet, ap = apparent, br = broad), coupling constant(s), integration. High-resolution mass spectra (HRMS) were obtained on a Bruker BioTOF II instrument. Purity of the final compounds was determined by ^1H NMR and reverse-phase HPLC and was 95%.

General Procedure A: EDC Coupling—To a solution of **42** (1.2 mmol, 1.20 equiv) and the corresponding carboxylic acid (1 mmol, 1.00 equiv) in DMF (7 mL) was added EDC (1 mmol, 1.00 equiv) followed by DMAP (1 mmol, 1.00 equiv) at 23 °C. The reaction was stirred for 16 h at 23 °C and quenched with water (25 mL). The mixture was extracted with EtOAc (3 × 50 mL). The combined organic layers were washed by saturated aqueous NaCl, dried (Na_2SO_4), filtered, and concentrated under reduced pressure. Purification by flash chromatography on silica gel (1:1 hexanes/EtOAc) afforded the coupled product.

1-(4-(4-(Benzo[d][1,3]dioxole-5-carbonyl)piperazin-1-yl)phenyl)ethanone 6—Compound **42** (98 mg, 0.48 mmol) was coupled with piperonylic acid (66 mg, 0.40 mmol) using general procedure A for EDC coupling. Purification by flash chromatography (1:1 hexanes/EtOAc) afforded the title compound (110 mg, 78%) as a white solid: mp 140–141 °C; R_f = 0.23 (1:1 hexanes/EtOAc); ^1H NMR (400 MHz, CDCl_3) δ 7.85 (d, J = 8.5 Hz, 2H), 6.94–6.91 (m, 2H), 6.85–6.79 (m, 3H), 5.97 (s, 2H), 3.73 (s, 4H), 3.35–3.33 (m, 4H), 2.48 (s, 3H); ^{13}C NMR (100 MHz, CDCl_3) δ 196.30, 169.8, 153.6, 148.9, 147.6, 130.2, 128.7, 128.2, 121.6, 113.8, 108.1, 107.9, 101.4, 47.5, 26.0; HRMS (ESI+) calcd for $\text{C}_{20}\text{H}_{20}\text{N}_2\text{NaO}_4^+$ 375.1315, found 375.1324 (error 2.4 ppm).

1-(4-(4-(2,3-Dihydrobenzo[b][1,4]dioxine-6-carbonyl)piperazin-1-yl)phenyl)ethanone 7—Compound **42** (98 mg, 0.48 mmol) was coupled with 1,4-benzodioxane-6-carboxylic acid (72 mg, 0.40 mmol) using general procedure A for EDC coupling. Purification by flash chromatography (1:1 hexanes/EtOAc) afforded the title compound (95 mg, 65%) as a white solid: mp 173–174 °C; R_f = 0.14 (1:1 hexanes/EtOAc); ^1H NMR (400 MHz, CDCl_3) δ 7.86 (d, J = 8.5 Hz, 2H), 6.98–6.91 (m, 2H), 6.88–6.84 (m, 3H), 4.26 (s, 4H), 3.75 (s, 4H), 3.35 (s, 4H), 2.50 (s, 3H); ^{13}C NMR (100 MHz, CDCl_3) δ 196.4, 169.9, 153.7, 145.1, 143.3, 130.3, 128.23, 128.16, 120.7, 117.2, 116.7, 113.8, 64.4, 64.2, 47.6, 26.1; HRMS (ESI+) calcd for $\text{C}_{21}\text{H}_{22}\text{N}_2\text{NaO}_4^+$ 389.1472, found 389.1462 (error 2.6 ppm).

1-(4-(4-(3,4-Dihydro-2H-benzo[b][1,4]dioxepine-7-carbonyl)piperazin-1-yl)phenyl)ethanone 8—Compound **42** (98 mg, 0.48 mmol) was coupled with 3,4-dihydro-2H-1,5-benzodioxepine-7-carboxylic acid (78 mg, 0.40 mmol) using general procedure A for EDC coupling. Purification by flash chromatography (1:1 hexanes/EtOAc) afforded the title compound (108 mg, 71%) as a white solid: mp 183–185 °C; R_f = 0.14 (1:1 hexanes/EtOAc); ^1H NMR (400 MHz, CDCl_3) δ 7.84 (d, J = 8.4 Hz, 2H), 7.05–6.97 (m, 3H), 6.83 (d, J = 8.5 Hz, 2H), 4.26–4.18 (m, 4H), 3.73 (s, 4H), 3.34 (s, 4H), 2.48 (s, 3H), 2.3–1.96 (m, 2H); ^{13}C NMR (100 MHz, CDCl_3) δ 196.3, 169.6, 153.6, 152.4, 150.7, 10.2, 130.0, 128.2, 122.3, 121.5, 120.8, 113.8, 70.4, 70.3, 47.5, 41.9, 31.2, 26.0; HRMS (ESI+) calcd for $\text{C}_{22}\text{H}_{24}\text{N}_2\text{NaO}_4^+$ 403.1628, found 403.1640 (error 3.0 ppm).

1-(4-(4-(3,4-Dichlorobenzoyl)piperazin-1-yl)phenyl)ethanone 9—Compound **42** (43 mg, 0.21 mmol) was coupled with 3,4-dichlorobenzoic acid (34 mg, 0.18 mmol) using general procedure A for EDC coupling. Purification by flash chromatography (1:1 hexanes/EtOAc) afforded the title compound (46 mg, 68%) as a white solid: mp 123–124 °C; R_f = 0.33 (1:1 hexanes/EtOAc); $^1\text{H NMR}$ (400 MHz, CDCl_3) δ 7.89–7.86 (m, 2H), 7.54–7.49 (m, 2H), 7.27 (dd, J = 8.3, 2.3 Hz, 1H), 6.88–6.85 (m, 2H), 3.86 (s, 2H), 3.63 (s, 2H), 3.37 (s, 4H), 2.52 (s, 3H); $^{13}\text{C NMR}$ (100 MHz, CDCl_3) δ 196.4, 167.9, 153.5, 135.0, 134.4, 133.1, 130.7, 130.3, 129.3, 128.6, 126.4, 114.1, 47.6, 42.2, 26.1; HRMS (ESI+) calcd for $\text{C}_{19}\text{H}_{18}\text{Cl}_2\text{N}_2\text{NaO}_2^+$ 399.0638, found 399.0630 (error 2.0 ppm).

1-(4-(4-(3,5-Dichlorobenzoyl)piperazin-1-yl)phenyl)ethanone 10—Compound **42** (98 mg, 0.48 mmol) was coupled with 3,5-dichlorobenzoic acid (76 mg, 0.40 mmol) using general procedure A for EDC coupling. Purification by flash chromatography (1:1 hexanes/EtOAc) afforded the title compound (105 mg, 70%) as a white solid: mp 194–195 °C; R_f = 0.41 (1:1 hexanes/EtOAc); $^1\text{H NMR}$ (400 MHz, CDCl_3) δ 7.87 (d, J = 8.5 Hz, 2H), 7.42 (d, J = 2.3 Hz, 1H), 7.31–7.30 (m, 2H), 6.86 (d, J = 8.5 Hz, 2H), 3.88 (s, 2H), 3.59 (s, 2H), 3.39 (s, 4H), 3.33 (s, 1H), 2.51 (s, 3H); $^{13}\text{C NMR}$ (100 MHz, CDCl_3) δ 196.4, 167.3, 153.5, 138.0, 135.5, 130.3, 130.0, 128.6, 125.5, 114.1, 47.9, 41.8, 26.1; HRMS (ESI+) calcd for $\text{C}_{19}\text{H}_{18}\text{Cl}_2\text{N}_2\text{NaO}_2^+$ 399.0638, found 399.0628 (error 2.5 ppm).

1-(4-(4-(3-Chloro-5-methoxybenzoyl)piperazin-1-yl)phenyl)ethanone 11—Compound **42** (98 mg, 0.48 mmol) was coupled with 3-chloro-5-methoxybenzoic acid (75 mg, 0.40 mmol) using general procedure A for EDC coupling. Purification by flash chromatography (1:1 hexanes/EtOAc) afforded the title compound (121 mg, 81%) as a white solid: mp 196–197 °C; R_f = 0.22 (1:1 hexanes/EtOAc); $^1\text{H NMR}$ (400 MHz, CDCl_3) δ 7.84 (d, J = 8.5 Hz, 2H), 6.95–6.92 (m, 2H), 6.84–6.82 (m, 3H), 3.85 (s, 2H), 3.85–3.78 (m, 5H), 3.56 (s, 2H), 3.35 (s, 4H), 2.48 (s, 3H); $^{13}\text{C NMR}$ (100 MHz, CDCl_3) δ 196.3, 168.5, 160.3, 153.5, 137.6, 135.1, 130.2, 128.3, 119.0, 115.6, 113.8, 111.2, 55, 47.6, 41.6, 26.0; HRMS (ESI+) calcd for $\text{C}_{20}\text{H}_{21}\text{ClN}_2\text{NaO}_3^+$ 395.1133, found 395.1143 (error 2.5 ppm).

1-(4-(4-(3-Chlorobenzoyl)piperazin-1-yl)phenyl)ethanone 12—Compound **44** (0.20 g, 0.90 mmol) was coupled with 4'-bromoacetophenone (0.15 g, 0.75 mmol) using general procedure B. Purification by flash chromatography (1:1 hexanes/EtOAc) afforded the title compound (0.18 g, 69%) as a white solid: mp 142–143 °C; R_f = 0.65 (EtOAc); $^1\text{H NMR}$ (400 MHz, CDCl_3) δ 7.89–7.86 (m, 2H), 7.43–7.29 (m, 4H), 6.88–6.84 (m, 2H), 3.89 (s, 2H), 3.60 (s, 2H), 3.37 (s, 4H), 2.51 (s, 3H); $^{13}\text{C NMR}$ (100 MHz, CDCl_3) δ 196.4, 168.8, 153.6, 137.0, 134.7, 130.3, 130.1, 130.0, 128.5, 127.3, 125.1, 114.0, 47.7 (br), 41.8 (br), 26.1; HRMS (ESI+) calcd for $\text{C}_{19}\text{H}_{19}\text{ClN}_2\text{NaO}_2^+$ 365.1027, found 365.1029 (error 0.5 ppm).

1-(4-(4-(5-Chloronicotinoyl)piperazin-1-yl)phenyl)ethanone 13—Compound **42** (98 mg, 0.48 mmol) was coupled with 5-chloronicotinic acid (63 mg, 0.40 mmol) using general procedure A for EDC coupling. Purification by flash chromatography (1:1 hexanes/EtOAc) afforded the title compound (90 mg, 66%) as a white solid: mp 161–162 °C; R_f = 0.13 (1:1 hexanes/EtOAc); $^1\text{H NMR}$ (400 MHz, CDCl_3) δ 8.64–8.58 (m, 1H), 8.53 (s, 1H),

7.85 (d, $J=8.5$ Hz, 2H), 7.76 (s, 1H), 6.84 (d, $J=8.5$ Hz, 2H), 3.89 (s, 2H), 3.62–3.57 (m, 2H), 3.43–3.31 (m, 4H), 2.48 (s, 3H); ^{13}C NMR (100 MHz, CDCl_3) δ 196.3, 166.1, 153.4, 149.9, 145.5, 134.7, 132.2, 131.9, 130.2, 128.6, 114.0, 47.1, 41.8, 26.1; HRMS (ESI+) calcd for $\text{C}_{18}\text{H}_{18}\text{ClN}_3\text{NaO}_2^+$ 366.0980, found 366.0967 (error 3.6 ppm).

1-(4-(4-Nicotinoylpiperazin-1-yl)phenyl)ethanone 14—Compound **42** (74 mg, 0.36 mmol) was coupled with nicotinic acid (37 mg, 0.30 mmol) using general procedure A for EDC coupling. Purification by flash chromatography (2:1 DCM/ CH_3CN) afforded the title compound (66 mg, 71%) as a white solid: mp 142–143 °C; $R_f=0.24$ (2:1 DCM– CH_3CN); ^1H NMR (400 MHz, CDCl_3) δ 8.68 (d, $J=5.2$ Hz, 2H), 7.88 (d, $J=8.5$ Hz, 2H), 7.78 (dt, $J=7.9, 1.9$ Hz, 1H), 7.38 (dd, $J=7.9, 5.0$ Hz, 1H), 6.87 (d, $J=8.6$ Hz, 2H), 3.92 (s, 2H), 3.62 (s, 2H), 3.39 (s, 4H), 2.51 (s, 3H); ^{13}C NMR (100 MHz, CDCl_3) δ 196.4, 167.8, 153.5, 151.0, 147.9, 135.1, 131.1, 130.3, 128.6, 123.5, 114.0, 47.6, 42.0, 26.1; HRMS (ESI+) calcd for $\text{C}_{18}\text{H}_{19}\text{N}_3\text{NaO}_2^+$ 332.1369, found 332.1360 (error 2.7 ppm).

1-(4-(4-(Thiazole-4-carbonyl)piperazin-1-yl)phenyl)ethanone 15—Compound **42** (74 mg, 0.36 mmol) was coupled with 4-thiazolecarboxylic acid (39 mg, 0.30 mmol) using general procedure A for EDC coupling. Purification by flash chromatography (EtOAc) afforded the title compound (68 mg, 72%) as a white solid: mp 118–119 °C; $R_f=0.24$ (EtOAc); ^1H NMR (400 MHz, CDCl_3) δ 8.79 (d, $J=2.1$ Hz, 1H), 8.05 (d, $J=2.2$ Hz, 1H), 7.87–7.85 (m, 2H), 6.85 (d, $J=8.9$ Hz, 2H), 4.10 (s, 2H), 3.92 (s, 2H), 3.41 (s, 4H), 2.49 (s, 3H); ^{13}C NMR (100 MHz, CDCl_3) δ 196.4, 162.3, 153.7, 151.9, 130.3, 128.1, 125.3, 113.6, 47.8, 47.1, 46.4, 42.3, 26.0; HRMS (ESI+) calcd for $\text{C}_{16}\text{H}_{17}\text{N}_3\text{NaO}_2\text{S}^+$ 338.0934, found 338.0928 (error 1.8 ppm).

1-(4-(4-(1-Methyl-1H-pyrazole-4-carbonyl)piperazin-1-yl)phenyl)ethanone 16—Compound **42** (74 mg, 0.36 mmol) was coupled with 1-methyl-1H-pyrazole-4-carboxylic acid (38 mg, 0.30 mmol) using general procedure A for EDC coupling. Purification by flash chromatography (1:4 DCM/ CH_3CN) afforded the title compound (68 mg, 73%) as a white solid: mp 170–171 °C; $R_f=0.18$ (1:4 DCM/ CH_3CN); ^1H NMR (400 MHz, CDCl_3) δ 7.86 (d, $J=8.0$, 2H), 7.72 (s, 1H), 7.62 (s, 1H), 6.84 (d, $J=8.0$, 2H), 3.89 (s, 3H), 3.85 (t, $J=4.0$ Hz, 4H), 3.38 (t, $J=4.0$ Hz, 4H), 2.48 (s, 3H); ^{13}C NMR (100 MHz, CDCl_3) δ 196.4, 167.8, 153.5, 151.0, 147.9, 135.1, 131.1, 130.3, 128.6, 123.5, 114.0, 47.7, 41.8, 26.1; HRMS (ESI+) calcd for $\text{C}_{17}\text{H}_{20}\text{N}_4\text{NaO}_2^+$ 335.1478, found 335.1477 (error 0.3 ppm).

1-(4-(4-Acetylphenyl)piperazin-1-yl)propan-1-one 17—Compound **42** (49 mg, 0.24 mmol) was coupled with propionic acid (0.015 mL, 0.20 mmol) using general procedure A for EDC coupling. Purification by flash chromatography (1:1 hexanes/EtOAc) afforded the title compound (42 mg, 81%) as a white solid: mp 75–76 °C; $R_f=0.07$ (1:1 hexanes/EtOAc); ^1H NMR (400 MHz, CDCl_3) δ 7.6 (d, $J=8$ Hz, 2H), 6.5 (d, $J=8$ Hz, 2H), 3.76 (d, $J=5.6$ Hz, 2H), 3.61 (d, $J=5.4$ Hz, 2H), 3.34 (dt, $J=12.1, 5.0$ Hz, 4H), 2.50 (d, $J=2.2$ Hz, 3H), 2.37 (qd, $J=7.5, 2.1$ Hz, 2H), 1.16 (td, $J=7.4, 2.2$ Hz, 3H); ^{13}C NMR (100 MHz, CDCl_3) δ 196.4, 172.3, 153.6, 130.3, 128.2, 113.7, 47.5, 47.3, 44.7, 40.9, 26.4, 26.1, 9.3; HRMS (ESI+) calcd for $\text{C}_{15}\text{H}_{20}\text{N}_2\text{NaO}_2^+$ 283.1417, found 283.1423 (error 2.1 ppm).

1-(4-(4-Acetylphenyl)piperazin-1-yl)butan-1-one 18—Compound **42** (49 mg, 0.24 mmol) was coupled with butyric acid (0.018 mL, 0.20 mmol) using general procedure A for EDC coupling. Purification by flash chromatography (1:1 hexanes/EtOAc) afforded the title compound (46 mg, 84%) as a white solid: mp 78–79 °C; R_f = 0.19 (1:1 hexanes/EtOAc); ^1H NMR (400 MHz, CDCl_3) δ 7.85 (d, J = 8.8 Hz, 2H), 6.84 (d, J = 8.9 Hz, 2H), 3.75 (t, J = 5.3 Hz, 2H), 3.62 (t, J = 5.2 Hz, 2H), 3.44–3.21 (m, 4H), 2.49 (s, 3H), 2.32 (t, J = 7.6 Hz, 2H), 1.63–1.69 (m, 2H), 0.96 (t, J = 8 Hz, 3H); ^{13}C NMR (100 MHz, CDCl_3) δ 196.3, 171.5, 153.6, 130.3, 128.1, 113.6, 47.58, 47.3, 44.9, 40.8, 35.0, 26.0, 18.6, 13.9; HRMS (ESI+) calcd for $\text{C}_{16}\text{H}_{22}\text{N}_2\text{NaO}_2^+$ 297.1573, found 297.1580 (error 2.4 ppm).

1-(4-(4-Acetylphenyl)piperazin-1-yl)hexan-1-one 19—Compound **42** (49 mg, 0.24 mmol) was coupled with hexanoic acid (0.025 mL, 0.20 mmol) using general procedure A for EDC coupling. Purification by flash chromatography (1:1 hexanes/EtOAc) afforded the title compound (52 mg, 86%) as a white solid: mp 73–74 °C; R_f = 0.20 (1:1 hexanes/EtOAc); ^1H NMR (400 MHz, CDCl_3) δ 7.84 (d, J = 8.4 Hz, 2H), 6.83 (d, J = 8.5 Hz, 2H), 3.74 (t, J = 5.2 Hz, 2H), 3.61 (t, J = 5.1 Hz, 2H), 3.32 (dt, J = 11.6, 5.1 Hz, 4H), 2.48 (s, 3H), 2.32 (t, J = 7.7 Hz, 2H), 1.62 (t, J = 7.4 Hz, 2H), 1.31 (d, J = 6.4 Hz, 4H), 0.87 (d, J = 6.3 Hz, 3H); ^{13}C NMR (100 MHz, CDCl_3) δ 196.3, 171.7, 153.6, 130.3, 128.1, 113.6, 47.5, 47.3, 44.9, 40.9, 33.1, 31.5, 26.1, 24.9, 22.4, 13.9; HRMS (ESI+) calcd for $\text{C}_{18}\text{H}_{26}\text{N}_2\text{NaO}_2^+$ 325.1886, found 325.1901 (error 4.6 ppm).

1-(4-(4-Acetylphenyl)piperazin-1-yl)-3-methylbutan-1-one 20—Compound **42** (49 mg, 0.24 mmol) was coupled with isovaleric acid (0.022 mL, 0.20 mmol) using general procedure A for EDC coupling. Purification by flash chromatography (1:1 hexanes/EtOAc) afforded the title compound (47 mg, 81%) as a white solid: mp 57–58 °C; R_f = 0.21 (1:1 hexanes/EtOAc); ^1H NMR (400 MHz, CDCl_3) δ 7.85 (d, J = 8 Hz, 2H), 6.84 (d, J = 8 Hz, 2H), 3.76 (t, J = 5.5 Hz, 2H), 3.63 (t, J = 4.0 Hz, 2H), 3.49–3.16 (m, 4H), 2.49 (s, 3H), 2.23 (dd, J = 7.0, 2.4 Hz, 2H), 2.12 (t, J = 6.5 Hz, 1H), 0.97 (dd, J = 6.6, 2.5 Hz, 6H); ^{13}C NMR (100 MHz, CDCl_3) δ 196.3, 171.0, 153.6, 130.3, 128.1, 113.7, 47.6, 47.3, 45.1, 41.9, 40.9, 26.1, 25.7, 22.6; HRMS (ESI+) calcd for $\text{C}_{17}\text{H}_{24}\text{N}_2\text{NaO}_2^+$ 311.1730, found 311.1738 (error 2.6 ppm).

(3-Chlorophenyl)(4-(4-(pyridin-2-yl)phenyl)piperazin-1-yl)-methanone 21—Compound **44** (92 mg, 0.41 mmol) was coupled with 2-(4-bromophenyl)pyridine (80 mg, 0.34 mmol) using general procedure B. Purification by flash chromatography (1:1 hexanes/EtOAc) afforded the title compound (73 mg, 57%) as a light brown solid: mp 158–159 °C; R_f = 0.19 (1:1 hexanes/EtOAc); ^1H NMR (400 MHz, CDCl_3) δ 8.64 (dt, J = 4.9, 1.4 Hz, 1H), 7.99–7.90 (m, 2H), 7.75–7.63 (m, 2H), 7.47–7.28 (m, 3H), 7.16 (ddd, J = 6.7, 4.8, 1.5 Hz, 1H), 7.05–6.96 (m, 3H), 3.94 (s, 2H), 3.61 (s, 2H), 3.34 (s, 2H), 3.25 (s, 2H); ^{13}C NMR (100 MHz, CDCl_3) δ 168.7, 156.8, 151.1, 149.4, 137.2, 136.6, 134.6, 131.1, 129.91, 129.87, 127.7, 127.2, 125.1, 121.2, 119.5, 116.1, 48.9 (br), 47.3, 42.0; HRMS (ESI+) calcd for $\text{C}_{22}\text{H}_{20}\text{ClN}_3\text{NaO}^+$ 400.1187, found 400.1176 (error 2.7 ppm).

(3-Chlorophenyl)(4-(5-methoxypyridin-2-yl)piperazin-1-yl)-methanone 22—Compound **44** (92 mg, 0.41 mmol) was coupled with 2-(4-bromophenyl)-5-methoxypyridine

(90 mg, 0.34 mmol) using general procedure B. Purification by flash chromatography (1:1 hexanes/EtOAc) afforded the title compound (71 mg, 51%) as a light brown solid: mp 165–166 °C; R_f = 0.70 (1:1 hexanes/EtOAc); ^1H NMR (400 MHz, CDCl_3) δ 8.34 (s, 1H), 7.86 (d, J = 8.3 Hz, 2H), 7.59 (d, J = 8.7 Hz, 1H), 7.46–7.28 (m, 5H), 6.98 (d, J = 8.4 Hz, 2H), 4.05–3.88 (m, 5H), 3.59 (s, 2H), 3.30 (s, 2H), 3.21 (s, 2H); ^{13}C NMR (100 MHz, CDCl_3) δ 168.7, 154.3, 150.6, 149.8, 137.2, 136.8, 134.6, 131.3, 130.0, 129.9, 127.3, 127.2, 125.1, 121.4, 119.9, 116.4, 55.6, 49.4, 47.4, 42.1; HRMS (ESI+) calcd for $\text{C}_{23}\text{H}_{22}\text{ClN}_3\text{NaO}_2^+$ 430.1293, found 430.1283 (error 2.3 ppm).

(3-Chlorophenyl)(4-(4-(3-methyl-1,2,4-oxadiazol-5-yl)phenyl)piperazin-1-yl)methanone 23—

Compound **44** (88 mg, 0.39 mmol) was coupled with 5-(4-bromophenyl)-3-methyl-1,2,4-oxadiazole (76 mg, 0.32 mmol) using general procedure B. Purification by flash chromatography (1:1 hexanes/EtOAc) afforded the title compound (44 mg, 36%) as a light brown solid: mp 195–196 °C; R_f = 0.21 (1:1 hexanes/EtOAc); ^1H NMR (400 MHz, CDCl_3) δ 8.07–7.96 (m, 2H), 7.48–7.26 (m, 4H), 7.00–6.91 (m, 2H), 3.92 (s, 2H), 3.63 (s, 2H), 3.39 (s, 4H), 2.44 (s, 3H); ^{13}C NMR (100 MHz, CDCl_3) δ 175.3, 168.9, 167.5, 153.3, 137.0, 134.7, 130.2, 130.0, 129.6, 127.3, 125.2, 114.9, 114.8, 47.7, 42.0; HRMS (ESI+) calcd for $\text{C}_{20}\text{H}_{19}\text{ClN}_4\text{NaO}_2^+$ 405.1089, found 405.1102 (error 3.2 ppm).

(3-Chlorophenyl)(4-(4-(1-methyl-1H-tetrazol-5-yl)phenyl)piperazin-1-yl)methanone 24—

Compound **44** (0.12 g, 0.55 mmol) was coupled with 5-(4-bromophenyl)-1-methyl-1H-tetrazole (0.11 g, 0.46 mmol) using general procedure B. Purification by flash chromatography (1:1 hexanes/EtOAc) afforded the title compound (0.12 g, 66%) as a light brown solid: mp 202–203 °C; R_f = 0.21 (1:1 hexanes/EtOAc); ^1H NMR (400 MHz, CDCl_3) δ 8.01 (d, J = 8.4 Hz, 2H), 7.42–7.27 (m, 4H), 6.96 (d, J = 8.4 Hz, 2H), 4.33 (s, 3H), 3.90 (s, 2H), 3.57 (s, 2H), 3.32 (s, 2H), 3.23 (s, 2H); ^{13}C NMR (100 MHz, CDCl_3) δ 168.7, 165.0, 151.9, 137.1, 134.6, 130.0, 129.9, 127.8, 127.2, 125.1, 118.8, 115.8, 48.7, 48.5, 47.1, 41.9, 39.3; HRMS (ESI+) calcd for $\text{C}_{19}\text{H}_{19}\text{ClN}_6\text{NaO}^+$ 405.1201, found 405.1216 (error 3.7 ppm).

(3-Chlorophenyl)(4-(4-(isoxazol-5-yl)phenyl)piperazin-1-yl)methanone 25—

The solution of **12** (50 mg, 0.15 mmol) and *N,N*-dimethylformamide dimethyl acetal (0.022 mL, 0.15 mmol) in *o*-xylene (2 mL) was refluxed for 8 h. After removing the solvent under reduced pressure, hydroxylamine hydrochloride (10 mg, 0.14 mmol) was added followed by EtOH (2 mL). The mixture was heated at 78 °C for 10 h. After cooling to 23 °C, H_2O (5 mL) was added. The mixture was extracted with EtOAc (3 \times 10 mL). The combined organic layers were washed by saturated aqueous NaCl, dried (Na_2SO_4), filtered, and concentrated under reduced pressure. Purification by flash chromatography on silica gel (1:1 hexanes/EtOAc) afforded the title compound (16 mg, 30%) as a light brown solid: mp 108–109 °C; R_f = 0.21 (1:1 hexanes/EtOAc); ^1H NMR (400 MHz, CDCl_3) δ 8.24 (d, J = 1.9 Hz, 1H), 7.74–7.68 (m, 2H), 7.46–7.35 (m, 3H), 7.32 (dt, J = 7.4, 1.5 Hz, 1H), 6.99–6.94 (m, 2H), 6.38 (d, J = 1.9 Hz, 1H), 3.92 (s, 2H), 3.60 (s, 2H), 3.32 (s, 4H); ^{13}C NMR (100 MHz, CDCl_3) δ 169.3, 168.8, 151.6, 150.8, 137.1, 134.7, 130.1, 130.0, 127.3, 127.2, 125.2, 119.2, 115.9, 97.1, 48.5, 47.4, 41.8; HRMS (ESI+) calcd for $\text{C}_{20}\text{H}_{18}\text{ClN}_3\text{NaO}_2^+$ 390.0980, found 390.0992 (error 3.1 ppm).

5-(4-(3-Chlorobenzoyl)piperazin-1-yl)-2,3-dihydro-1H-inden-1-one 26—

Compound **44** (31 mg, 0.14 mmol) was coupled with 5-bromo-1-indanone (25 mg, 0.12 mmol) using general procedure B. Purification by flash chromatography (1:1 hexanes/EtOAc) afforded the title compound (32 mg, 76%) as a light brown oil: R_f = 0.21 (1:1 hexanes/EtOAc); ^1H NMR (400 MHz, CDCl_3) δ 7.65 (d, J = 8.6 Hz, 1H), 7.47–7.30 (m, 4H), 6.87 (dd, J = 8.7, 2.2 Hz, 1H), 6.82 (d, J = 2.1 Hz, 1H), 3.89 (s, 2H), 3.63 (s, 2H), 3.42 (s, 4H), 3.06–3.03 (m, 2H), 2.66–2.63 (m, 2H); ^{13}C NMR (100 MHz, CDCl_3) δ 205.0, 168.9, 157.8, 155.3, 136.9, 134.7, 130.2, 130.0, 128.8, 127.3, 125.2, 114.9, 110.6, 77.2, 47.9, 42.0, 36.4, 25.9; HRMS (ESI+) calcd for $\text{C}_{20}\text{H}_{19}\text{ClN}_2\text{NaO}_2^+$ 377.1027, found 377.1017 (error 2.7 ppm).

5-(4-(3-Chlorobenzoyl)piperazin-1-yl)isobenzofuran-1(3H)-one 27—

Compound **44** (154 mg, 0.68 mmol) was coupled with 5-bromophthalide (121 mg, 0.57 mmol) using general procedure B. Purification by flash chromatography (1:1 hexanes/EtOAc) afforded the title compound (81 mg, 40%) as a light brown solid: mp 154–155 °C; R_f = 0.11 (1:1 hexanes/EtOAc); ^1H NMR (400 MHz, CDCl_3) δ 7.75 (d, J = 8.6 Hz, 1H), 7.47–7.33 (m, 3H), 7.35–7.24 (m, 1H), 6.99 (dd, J = 8.7, 2.1 Hz, 1H), 6.82 (d, J = 2.1 Hz, 1H), 5.20 (s, 2H), 3.92 (s, 2H), 3.64 (s, 2H), 3.41 (s, 4H); ^{13}C NMR (100 MHz, CDCl_3) δ 168.8, 154.9, 149.2, 136.8, 134.7, 130.2, 130.0, 127.2, 126.8, 125.1, 116.2, 116.0, 106.4, 69.1, 47.97, 47.0, 41.8; HRMS (ESI+) calcd for $\text{C}_{19}\text{H}_{17}\text{ClN}_2\text{NaO}_3^+$ 379.0820, found 379.0804 (error 4.2 ppm).

5-(4-(3-Chlorobenzoyl)piperazin-1-yl)-2-methylisindolin-1-one 28—

Compound **44** (72 mg, 0.32 mmol) was coupled with 5-bromo-2-methylisindolin-1-one (60 mg, 0.26 mmol) using general procedure B. Purification by flash chromatography (1:1 hexanes/EtOAc) afforded the title compound (43 g, 45%) as a light brown solid: mp 155–156 °C; R_f = 0.11 (1:1 hexanes/EtOAc); ^1H NMR (400 MHz, CDCl_3) δ 7.69 (d, J = 8.4 Hz, 1H), 7.43–7.26 (m, 4H), 6.97 (dd, J = 8.5, 2.2 Hz, 1H), 6.89 (d, J = 2.1 Hz, 1H), 4.29 (s, 2H), 3.92 (s, 2H), 3.60 (s, 2H), 3.30 (s, 4H), 3.14 (s, 3H); ^{13}C NMR (100 MHz, CDCl_3) δ 168.8, 168.6, 153.4, 143.0, 137.1, 134.7, 130.1, 130.0, 127.3, 125.2, 124.8, 124.5, 116.1, 109.3, 51.9, 49.1, 47.5, 42.1, 29.4; HRMS (ESI+) calcd for $\text{C}_{20}\text{H}_{20}\text{ClN}_3\text{NaO}_2^+$ 392.1136, found 392.1146 (error 2.6 ppm).

(3-Chlorophenyl)(4-(1,3-dihydroisobenzofuran-5-yl)piperazin-1-yl)methanone 29—

Compound **44** (112 mg, 0.50 mmol) was coupled with 5-bromo-1,3-dihydroisobenzofuran (84 mg, 0.42 mmol) using general procedure B. Purification by flash chromatography (1:1 hexanes/EtOAc) afforded the title compound (78 mg, 54%) as a light brown oil: R_f = 0.32 (1:1 hexanes/EtOAc); ^1H NMR (400 MHz, CDCl_3) δ 7.42–7.29 (m, 4H), 7.13 (d, J = 8.2 Hz, 1H), 6.85 (dd, J = 8.2, 2.2 Hz, 1H), 6.80 (d, J = 2.2 Hz, 1H), 5.05 (q, J = 2.4 Hz, 4H), 3.92 (s, 2H), 3.58 (s, 2H), 3.20 (s, 3H), 3.12 (s, 2H); ^{13}C NMR (100 MHz, CDCl_3) δ 168.7, 150.8, 140.5, 137.2, 134.6, 131.5, 129.93, 129.89, 127.2, 125.1, 121.5, 116.6, 109.5, 73.5, 73.2, 50.3, 47.6, 42.1; HRMS (ESI+) calcd for $\text{C}_{19}\text{H}_{19}\text{ClN}_2\text{NaO}_2^+$ 365.1027, found 365.1014 (error 3.6 ppm).

1-(3-(4-(3-Chlorobenzoyl)piperazin-1-yl)phenyl)ethanone 30—Compound **44** (121 mg, 0.54 mmol) was coupled with 3'-bromoacetophenone (0.06 mL, 0.45 mmol) using general procedure B. Purification by flash chromatography (1:1 hexanes/EtOAc) afforded the title compound (56 mg, 36%) as a light brown oil: R_f = 0.34 (1:1 hexanes/EtOAc); ^1H NMR (400 MHz, CDCl_3) δ 7.51–7.29 (m, 7H), 7.11 (dd, J = 8.3, 2.5 Hz, 1H), 3.91 (s, 2H), 3.58 (s, 2H), 3.28 (s, 2H), 3.20 (s, 2H), 2.57 (s, 3H); ^{13}C NMR (100 MHz, CDCl_3) δ 198.2, 168.7, 151.0, 138.0, 137.1, 134.6, 130.0, 129.9, 129.4, 127.2, 125.1, 121.3, 120.8, 115.3, 49.4, 47.3 (br), 42.0, 26.7; HRMS (ESI+) calcd for $\text{C}_{19}\text{H}_{19}\text{ClN}_2\text{NaO}_2^+$ 365.1027, found 365.1038 (error 3.0 ppm).

Methyl 4-(4-(3-Chlorobenzoyl)piperazin-1-yl)benzoate 31—Compound **44** (202 mg, 0.90 mmol) was coupled with methyl 4-bromobenzoate (161 mg, 0.75 mmol) using general procedure B. Purification by flash chromatography (1:1 hexanes/EtOAc) afforded the title compound (201 mg, 75%) as a light brown solid: mp 165–165 °C; R_f = 0.37 (1:1 hexanes/EtOAc); ^1H NMR (400 MHz, CDCl_3) δ 7.93–7.89 (m, 2H), 7.41–7.26 (m, 4H), 6.86–6.83 (m, 2H), 3.83 (s, 5H), 3.56 (s, 2H), 3.33 (s, 4H); ^{13}C NMR (100 MHz, CDCl_3) δ 168.7, 166.8, 153.5, 137.0, 134.5, 131.1, 130.0, 129.9, 127.2, 125.1, 120.6, 114.1, 51.6, 47.8, 47.1, 41.9; HRMS (ESI+) calcd for $\text{C}_{19}\text{H}_{19}\text{ClN}_2\text{NaO}_3^+$ 381.0976, found 381.0961 (error 3.9 ppm).

4-(4-(3-Chlorobenzoyl)piperazin-1-yl)benzonitrile 32—Compound **44** (154 mg, 0.68 mmol) was coupled with 4-bromobenzonitrile (104 mg, 0.57 mmol) using general procedure B. Purification by flash chromatography (1:1 hexanes/EtOAc) afforded the title compound (157 mg, 85%) as a light brown oil: R_f = 0.35 (1:1 hexanes/EtOAc); ^1H NMR (400 MHz, CDCl_3) δ 7.49–7.46 (m, 2H), 7.41–7.33 (m, 3H), 7.30–7.27 (m, 1H), 6.86–6.83 (m, 2H), 3.86 (s, 2H), 3.58 (s, 2H), 3.34 (s, 4H); ^{13}C NMR (100 MHz, CDCl_3) δ 168.6, 152.7, 136.7, 134.5, 133.3, 130.0, 129.8, 127.1, 125.0, 119.5, 114.5, 101.0, 47.2, 41.5; HRMS (ESI+) calcd for $\text{C}_{18}\text{H}_{16}\text{ClN}_3\text{NaO}^+$ 348.0874, found 348.0892 (error 5.2 ppm).

(3-Chlorophenyl)(4-(4-nitrophenyl)piperazin-1-yl)methanone 33—Compound **44** (124 mg, 0.55 mmol) was coupled with 1-bromo-4-nitrobenzene (92 mg, 0.46 mmol) using general procedure B. Purification by flash chromatography (1:1 hexanes/EtOAc) afforded the title compound (119 mg, 75%) as a yellow solid: mp 102–103 °C; R_f = 0.40 (1:1 hexanes/EtOAc); ^1H NMR (400 MHz, CDCl_3) δ 8.11 (d, J = 8 Hz, 2H), 7.42–7.32 (m, 4H), 6.83 (d, J = 8 Hz, 2H), 3.89 (s, 2H), 3.63 (s, 2H), 3.45 (s, 4H); ^{13}C NMR (100 MHz, CDCl_3) δ 168.7, 154.2, 138.8, 136.7, 134.5, 130.1, 129.9, 127.2, 125.7, 125.0, 112.9, 46.8, 41.6; HRMS (ESI+) calcd for $\text{C}_{17}\text{H}_{16}\text{ClN}_3\text{NaO}_3^+$ 368.0772, found 368.0786 (error 3.8 ppm).

1-(5-(4-(3-Chlorobenzoyl)piperazin-1-yl)thiophen-2-yl)ethanone 34—Compound **44** (154 mg, 0.68 mmol) was coupled with 2-acetyl-5-bromothiophene (117 mg, 0.57 mmol) using general procedure B. Purification by flash chromatography (1:1 hexanes/EtOAc) afforded the title compound (119 mg, 60%) as a light brown solid: mp 131–132 °C; R_f = 0.25 (1:1 hexanes/EtOAc); ^1H NMR (400 MHz, CDCl_3) δ 7.47–7.32 (m, 4H), 7.31–7.25 (m, 1H), 6.07 (dd, J = 4.3, 1.3 Hz, 1H), 3.86 (s, 2H), 3.62 (s, 2H), 3.32 (s, 4H), 2.41 (s, 3H); ^{13}C NMR (100 MHz, CDCl_3) δ 189.1, 168.8, 165.8, 136.7, 134.73, 134.68, 130.2,

130.0, 129.8, 127.2, 125.1, 105.1, 49.7, 46.5, 41.3, 25.2; HRMS (ESI+) calcd for $C_{17}H_{17}ClN_2NaO_2S^+$ 371.0591, found 371.0610 (error 5.1 ppm).

(3-Chlorophenyl)(4-(4-(1-(hydroxyimino)ethyl)phenyl)piperazin-1-yl)methanone

35—To a solution of **12** (177 mg, 0.51 mmol) in EtOH (2 mL) was added DIPEA (0.14 mL, 0.82 mmol) and hydroxylamine hydrochloride (57 mg, 0.82 mmol). The mixture was heated at 60 °C for 2 h. After cooling, EtOH was removed in vacuo, and then H₂O (20 mL) was added. The mixture was extracted with EtOAc (3 × 20 mL). The combined organic layers were washed by saturated aqueous NaCl, dried (Na₂SO₄), filtered, and concentrated under reduced pressure. Purification by flash chromatography on silica gel (EtOAc) afforded the title compound (60 mg, 33%) as a white solid: mp 180–181 °C; R_f = 0.74 (EtOAc); ¹H NMR (400 MHz, CDCl₃) δ 8.95 (s, 1H), 7.58–7.55 (m, 2H), 7.44–7.30 (m, 4H), 6.91–6.88 (m, 2H), 3.93 (s, 2H), 3.59 (s, 2H), 3.29 (s, 2H), 3.20 (s, 2H), 2.25 (s, 3H); ¹³C NMR (100 MHz, CDCl₃) δ 168.8, 155.3, 151.2, 137.1, 130.0, 129.9, 128.4, 127.3, 127.0, 125.2, 115.9, 49.1, 47.3, 42.1, 11.9; HRMS (ESI+) calcd for $C_{19}H_{20}ClN_3NaO_2^+$ 380.1136, found 380.1156 (error 5.3 ppm).

5-(4-(Benzo[d][1,3]dioxole-5-carbonyl)piperazin-1-yl)-2,3-dihydro-1H-inden-1-one

36—Compound **43** (212 mg, 0.98 mmol) was coupled with piperonylic acid (132 mg, 0.82 mmol) using general procedure A for EDC coupling. Purification by flash chromatography (EtOAc) afforded the title compound (218 mg, 73%) as a white solid: mp 158–159 °C; R_f = 0.43 (EtOAc); ¹H NMR (400 MHz, CDCl₃) δ 7.61 (d, J = 8.0 Hz, 1H), 6.94–6.90 (m, 2H), 6.85–6.78 (m, 3H), 5.97 (s, 2H), 3.74 (s, 4H), 3.37 (s, 4H), 3.01–2.98 (m, 2H), 2.60–2.58 (m, 2H); ¹³C NMR (100 MHz, CDCl₃) δ 204.8, 169.8, 157.7, 155.3, 149.0, 147.6, 128.7, 128.4, 125.0, 121.6, 114.6, 110.3, 108.1, 108.0, 101.4, 47.7, 36.3, 25.8; HRMS (ESI+) calcd for $C_{21}H_{20}N_2NaO_4^+$ 387.1315, found 387.1326 (error 2.8 ppm).

1-(4-(1-(3-Chlorobenzyl)-1H-1,2,3-triazol-4-yl)phenyl)ethanone

37—To a solution of **46**⁴⁴ (84.0 mg, 0.50 mmol, 1.00 equiv) and 1-(4-ethynylphenyl)ethanone (72 mg, 0.50 mmol) in EtOH/H₂O (1:1, 6 mL) were added CuSO₄·5H₂O (12.0 mg, 0.05 mmol, 0.10 equiv) in one portion followed by sodium ascorbate (30.0 mg, 0.15 mmol, 0.30 equiv) in one portion at 23 °C. The resulting yellowish cloudy suspension was stirred for 12 h at 23 °C; 10 mL of cold 1:1 hexanes/EtOAc was added for trituration, and the suspension was filtered to afford the title compound (105 mg, 68%) as a light brown solid: mp 164–165 °C; ¹H NMR (400 MHz, DMSO-*d*₆) δ 8.68 (s, 1H), 8.14 (t, J = 1.9 Hz, 1H), 8.08–8.02 (m, 5H), 7.84 (dt, J = 7.6, 1.4 Hz, 1H), 7.67 (t, J = 7.9 Hz, 1H), 6.32 (s, 2H), 2.61 (s, 3H); ¹³C NMR (100 MHz, DMSO-*d*₆) δ 191.3, 145.4, 135.94, 135.88, 135.0, 134.0, 133.9, 131.0, 129.0, 128.0, 126.9, 125.1, 124.2, 56.2, 26.7; HRMS (ESI+) calcd for $C_{17}H_{14}ClN_3NaO^+$ 334.0718, found 334.0722 (error 1.2 ppm).

1-(5-(1-(3-Chlorobenzyl)-1H-1,2,3-triazol-4-yl)thiophen-2-yl)ethanone

38—Using the procedure for the synthesis of **37**, compound **46** (97 mg, 0.58 mmol) was reacted with 1-(5-ethynylthiophen-2-yl)ethanone (88 mg, 0.58 mmol). Purification by adding 10 mL of cold 1:1 hexanes/EtOAc for trituration followed by filtration afforded the title compound (128 mg, 70%) as a light brown solid: mp 174–175 °C; ¹H NMR (400 MHz, DMSO-*d*₆) δ

8.62 (s, 1H), 8.12 (t, $J = 1.9$ Hz, 1H), 8.04 (d, $J = 7.8$ Hz, 1H), 7.96 (d, $J = 3.9$ Hz, 1H), 7.84–7.79 (m, 1H), 7.67 (t, $J = 7.9$ Hz, 1H), 7.60 (d, $J = 3.9$ Hz, 1H), 6.32 (s, 2H), 2.56 (s, 3H); ^{13}C NMR (100 MHz, DMSO- d_6) δ 191.2, 190.7, 142.5, 140.9, 135.8, 134.9, 134.0, 133.9, 131.0, 128.0, 126.9, 125.3, 123.9, 56.3, 26.5; HRMS (ESI+) calcd for $\text{C}_{15}\text{H}_{12}\text{ClN}_3\text{NaOS}^+$ 340.0282, found 340.0291 (error 2.6 ppm).

1-(4-(4-(3-Chlorobenzoyl)piperidin-1-yl)phenyl)ethanone 39—The mixture of **49** (61 mg, 0.19 mmol) in 4 mL of 1:3 TFA/ CH_2Cl_2 was stirred at rt for 3 h. After removing the solvent under reduced pressure, the residue was coupled with 1-(4-bromophenyl)ethanone (24 mg, 0.12 mmol) using general procedure B. Purification by flash chromatography (1:1 hexanes/EtOAc) afforded the title compound (28 mg, 68%) as a white solid: mp 121–122 °C; $R_f = 0.33$ (2:1 hexanes/EtOAc); ^1H NMR (400 MHz, CDCl_3) δ 7.92–7.82 (m, 4H), 7.56 (d, $J = 8.0$ Hz, 1H), 7.45 (t, $J = 8.0$ Hz, 1H), 6.89 (d, $J = 8.0$ Hz, 2H), 3.96 (d, $J = 9.0$ Hz, 2H), 3.46–3.41 (m, 1H), 3.10–3.03 (m, 2H), 2.51 (s, 3H), 2.04–1.84 (m, 4H); ^{13}C NMR (100 MHz, CDCl_3) δ 200.6, 196.4, 153.9, 137.4, 135.1, 133.1, 130.4, 130.1, 128.3, 127.4, 126.3, 113.6, 47.3, 43.3, 27.8, 26.1; HRMS (ESI+) calcd for $\text{C}_{20}\text{H}_{20}\text{ClNNaO}_2^+$ 364.1075, found 364.1069 (error 1.6 ppm).

1-(4-(4-(Benzo[d][1,3]dioxole-5-carbonyl)piperidin-1-yl)phenyl)-ethanone 40—The mixture of **50** (63 mg, 0.19 mmol) in 4 mL of 1:3 TFA/ CH_2Cl_2 was stirred at rt for 3 h. After removing the solvent under reduced pressure, the residue was coupled with 1-(4-bromophenyl)ethanone (24 mg, 0.12 mmol) using general procedure B. Purification by flash chromatography (1:1 hexanes/EtOAc) afforded the title compound (26 mg, 62%) as a white solid: mp 170–171 °C; $R_f = 0.30$ (2:1 hexanes/EtOAc); ^1H NMR (400 MHz, CDCl_3) δ 7.88 (d, $J = 8.0$ Hz, 2H), 7.59 (dd, $J = 8.0, 4.0$ Hz, 1H), 7.44 (d, $J = 4.0$ Hz, 1H), 6.89 (dd, $J = 8.0, 4.0$ Hz, 3H), 6.05 (s, 2H), 3.98 (dt, $J = 12.0, 4.0$ Hz, 2H), 3.42–3.37 (m, 1H), 3.07 (td, $J = 12.0, 4.0$ Hz, 2H), 2.52 (s, 3H), 1.98–1.88 (m, 4H); ^{13}C NMR (100 MHz, CDCl_3) δ 199.9, 196.4, 154.0, 151.8, 148.4, 130.5, 130.4, 124.3, 113.6, 108.1, 108.0, 101.9, 47.4, 43.0, 28.2, 26.1; HRMS (ESI+) calcd for $\text{C}_{21}\text{H}_{21}\text{NNaO}_4^+$ 374.1363, found 374.1370 (error 1.9 ppm).

1-(4-(Piperazin-1-yl)phenyl)ethanone 42—To a solution of piperazine **41** (775 mg, 9.00 mmol, 3.00 equiv) in DMSO (12 mL) was added 4'-fluoroacetophenone (0.36 mL, 3.00 mmol, 1.00 equiv), and the mixture was heated at 110 °C for 24 h. After cooling to 23 °C, the reaction mixture was quenched with water (50 mL). The mixture was extracted with EtOAc (3 \times 30 mL). The combined organic layers were washed by saturated aqueous NaCl, dried (Na_2SO_4), filtered, and concentrated under reduced pressure. Purification by flash chromatography on silica gel (130:25:4 $\text{CHCl}_3/\text{MeOH}/\text{NH}_4\text{OH}$) afforded the title compound (531 mg, 84%) as a light yellow solid: mp 102–103 °C; $R_f = 0.30$ (130:25:4 $\text{CHCl}_3/\text{MeOH}/\text{NH}_4\text{OH}$); ^1H NMR (400 MHz, CDCl_3) δ 7.86 (d, $J = 8.9$ Hz, 2H), 6.85 (d, $J = 8.7$ Hz, 2H), 3.33–3.30 (m, 4H), 3.04–3.01 (m, 4H), 2.51 (s, 3H), 2.03 (s, 1H); ^{13}C NMR (100 MHz, CDCl_3) δ 196.5, 154.5, 130.3, 127.6, 113.4, 48.4, 45.8, 26.1.

(3-Chlorophenyl)(piperazin-1-yl)methanone 44—To a solution of piperazine **41** (1.00 g, 11.6 mmol, 1.05 equiv) in THF (50 mL) was added *n*-BuLi (2.5 M in hexanes, 10.2 mL, 25.5 mmol, 2.32 equiv) at 23 °C. The reaction was stirred for 1 h at 23 °C, and then 3-

chlorobenzoyl chloride (1.41 mL, 11.0 mmol, 1.00 equiv) was added. After 10 min, the reaction mixture was quenched with MeOH (20 mL) and concentrated under reduced pressure. The residue was partitioned between EtOAc (50 mL) and saturated aqueous NaHCO₃ (50 mL). The aqueous layer was extracted with EtOAc (2 × 30 mL). The combined organic layers were washed by saturated aqueous NaCl, dried (Na₂SO₄), filtered, and concentrated under reduced pressure. Purification by flash chromatography on silica gel (130:25:4 CHCl₃/MeOH/NH₄OH) afforded the title compound (1.60 g, 65%) as a light brown solid: mp 86–87 °C; *R*_f = 0.43 (130:25:4 CHCl₃/MeOH/NH₄OH); ¹H NMR (400 MHz, CDCl₃) δ 7.43–7.30 (m, 3H), 7.31–7.23 (m, 1H), 3.74 (br s, 2H), 3.37 (br s, 2H), 2.93 (br s, 2H), 2.82 (br s, 2H), 1.71 (s, 1H); ¹³C NMR (100 MHz, CDCl₃) δ 167.9, 137.1, 133.8, 129.3, 129.0, 126.5, 124.4, 48.3, 45.7, 45.2, 42.6; HRMS (ESI+) calcd for C₁₁H₁₃ClN₂NaO⁺ 247.0609, found 247.0615 (error 2.4 ppm).

General Procedure B: Palladium-Catalyzed Coupling—A mixture of **44** (1 mmol, 1.20 equiv), aryl bromide (0.82 mmol, 1.00 equiv), Cs₂CO₃ (1.64 mmol, 2.00 equiv), Pd₂(dba)₃ (0.033 mmol, 0.04 equiv), and BINAP (0.066 mmol, 0.08 equiv) in toluene (6 mL) was purged with argon for 3 min. The reaction mixture was heated at 100 °C for 16 h. After cooling to 23 °C, H₂O (20 mL) was added. The mixture was extracted with EtOAc (3 × 20 mL). The combined organic layers were washed by saturated aqueous NaCl, dried (Na₂SO₄), filtered, and concentrated under reduced pressure. Purification by flash chromatography on silica gel (1:1 hexanes/EtOAc) afforded the coupled product.

tert-Butyl 4-(3-Chlorobenzoyl)piperidine-1-carboxylate 49—To the solution of 1-bromo-3-chlorobenzene (0.12 mL, 1 mmol) in THF (5 mL) at –78 °C was added 2.5 M *t*-BuLi (0.44 mL, 1.1 mmol). The mixture was stirred at –78 °C for 30 min, and **48**⁴⁵ (245 mg, 0.9 mmol) was added. The mixture was slowly warmed to rt, stirred for 16 h, and quenched by adding H₂O (10 mL). The mixture was extracted with EtOAc (3 × 20 mL). The combined organic layers were washed by saturated aqueous NaCl, dried (Na₂SO₄), filtered, and concentrated under reduced pressure. Purification by flash chromatography on silica gel (5:1 hexanes/EtOAc) afforded the title compound (183 mg, 57%) as a white solid: *R*_f = 0.23 (5:1 hexanes/EtOAc); ¹H NMR (400 MHz, CDCl₃) δ 7.89 (s, 1H), 7.81 (d, *J* = 8.0 Hz, 1H), 7.55 (d, *J* = 8.0 Hz, 1H), 7.40–7.44 (m, 1H), 4.15 (s, 2H), 3.38 (tt, *J* = 12.0, 4.0 Hz, 1H), 2.93 (t, *J* = 12.0 Hz, 2H), 1.84–1.81 (m, 2H), 1.73–1.64 (m, 2H), 1.46 (s, 9H); ¹³C NMR (100 MHz, CDCl₃) δ 200.7, 171.9, 154.6, 137.4, 135.1, 133.0, 130.1, 128.3, 126.3, 79.7, 43.6, 43.3, 28.4.

tert-Butyl 4-(Benzo[d][1,3]dioxole-5-carbonyl)piperidine-1-carboxylate 50—To the solution of 5-bromobenzo[d][1,3]dioxole (0.12 mL, 1 mmol) in THF (5 mL) at –78 °C was added 1.7 M *t*-BuLi (1.3 mL, 2.2 mmol). The mixture was stirred at –78 °C for 30 min, and **48**³⁰ (245 mg, 0.9 mmol) was added. The mixture was warmed to rt slowly and stirred for 16 h. The reaction was quenched by the addition of H₂O (10 mL). The mixture was extracted with EtOAc (3 × 20 mL). The combined organic layers were washed by saturated aqueous NaCl, dried (Na₂SO₄), filtered, and concentrated under reduced pressure. Purification by flash chromatography on silica gel (5:1 hexanes/EtOAc) afforded the title compound (161 mg, 54%) as a white solid: *R*_f = 0.16 (5:1 hexanes/EtOAc); ¹H NMR (400

MHz, CDCl₃) δ 7.47 (d, J = 8.0 Hz, 1H), 7.32 (s, 1H), 6.77 (d, J = 8.0 Hz, 1H), 5.95 (s, 2H), 4.09–4.06 (m, 2H), 3.27–3.21 (m, 1H), 2.83–2.77 (m, 2H), 1.74–1.71 (m, 2H), 1.64–1.58 (m, 2H), 1.38 (s, 9H); ¹³C NMR (100 MHz, CDCl₃) δ 199.8, 154.4, 151.6, 148.1, 130.3, 124.1, 107.8, 107.7, 101.7, 79.3, 53.2, 43.0, 28.4, 28.2.

Supplementary Material

Refer to Web version on PubMed Central for supplementary material.

Acknowledgments

This work was supported by NIH Grant AI091790. Isothermal titration calorimetry was carried out using an ITC-200 microcalorimeter funded in part by the NIH Shared Instrumentation Grant S10-OD017982. This research used resources at the Industrial Macromolecular Crystallography Association Collaborative Access Team (IMCA-CAT) beam-line 17-ID supported by the companies of the Industrial Macromolecular Crystallography Association through a contract with Hauptman-Woodward Medical Research Institute. This research also used resources of the Advanced Photon Source, a U.S. Department of Energy (DOE) Office of Science User Facility operated for the DOE Office of Science by Argonne National Laboratory under Contract No. DE-AC02-06CH11357. The authors also acknowledge the use of beamline 4.2.2 (Molecular Biology Consortium) at the Advanced Light Source and thank the beamline director, Jay Nix. This research used resources of the Advanced Light Source, which is a DOE Office of Science User Facility under contract no. DE-AC02-05CH11231.

ABBREVIATIONS USED

AMTOB	<i>S</i> -adenosyl-2-oxo-4-methylthiobutyric acid
BINAP	2,2'-bis(diphenylphosphino)-1,1'-binaphthyl
Boc	<i>N</i> -tert-butoxycarbonyl
DAPA	7,8-diaminopelargonic acid
DIPEA	<i>N,N</i> -diisopropylethylamine
DMAP	4-dimethylaminopyridine
DOA	5'-deoxyadenosine
EDC	1-ethyl-3-(3-(dimethylamino)-propyl)carbodiimide
KAPA	7-keto-8-aminopelargonic acid
ITC	isothermal titration calorimetry
Mtb	<i>Mycobacterium tuberculosis</i>
PLP	pyridoxal 5'-phosphate
SAM	<i>S</i> -adenosylmethionine
TB	tuberculosis
TFA	trifluoroacetic acid
WT	wild-type

References

1. Daniel TM. The History of Tuberculosis. *Respir Med.* 2006; 100(11):1862–1870. [PubMed: 16949809]
2. Comas I, Coscolla M, Luo T, Borrell S, Holt KE, Kato-Maeda M, Parkhill J, Malla B, Berg S, Thwaites G, Yeboah-Manu D, Bothamley G, Mei J, Wei L, Bentley S, Harris SR, Niemann S, Diel R, Aseffa A, Gao Q, Young D, Gagneux S. Out-of-Africa Migration and Neolithic Coexpansion of Mycobacterium Tuberculosis with Modern Humans. *Nat Genet.* 2013; 45(10):1176–1182. [PubMed: 23995134]
3. Nerlich AG, Haas CJ, Zink A, Szeimies U, Hagedorn HG. Molecular Evidence for Tuberculosis in an Ancient Egyptian Mummy. *Lancet.* 1997; 350(9088):1404.
4. Salo WL, Aufderheide AC, Buikstra J, Holcomb TA. Identification of Mycobacterium Tuberculosis DNA in a Pre-Columbian Peruvian Mummy. *Proc Natl Acad Sci USA.* 1994; 91(6):2091–2094. [PubMed: 8134354]
5. World Health Organization. Global Tuberculosis Report 2016. Geneva, Switzerland: 2016.
6. UNAIDS. UNAIDS Fact Sheet November 2016. Geneva, Switzerland: 2016. Joint United Nations Programme on HIV/AIDS.
7. Uplekar M, Weil D, Lonroth K, Jaramillo E, Lienhardt C, Dias HM, Falzon D, Floyd K, Gargioni G, Getahun H, Gilpin C, Glaziou P, Grzemska M, Mirzayev F, Nakatani H, Raviglione M. WHO's New End TB Strategy. *Lancet.* 2015; 385(9979):1799–1801. [PubMed: 25814376]
8. World Health Organization. Treatment of Tuberculosis Guidelines. 4th. Geneva, Switzerland: 2010.
9. Espinal MA. The Global Situation of MDR-TB. *Tuberculosis.* 2003; 83(1–3):44–51. [PubMed: 12758188]
10. World Health Organization. Drug-Resistant TB: Surveillance and Response: Supplement to Global Tuberculosis Report 2014. Geneva, Switzerland: 2014.
11. World Health Organization. Multidrug and Extensively Drug-Resistant TB (M/XDR-TB): 2010 Global Report on Surveillance and Response. World Health Organization; Geneva, Switzerland: 2010.
12. Dheda K, Migliori GB. The Global Rise of Extensively Drug-Resistant Tuberculosis: Is the Time to Bring Back Sanatoria Now Overdue? *Lancet.* 2012; 379(9817):773–775. [PubMed: 22033020]
13. Migliori GB, Besozzi G, Girardi E, Kliiman K, Lange C, Toungoussova OS, Ferrara G, Cirillo DM, Gori A, Matteelli A, Spanevello A, Codecasa LR, Raviglione MC, SMIRA/TBNET Study Group. Clinical and Operational Value of the Extensively Drug-Resistant Tuberculosis Definition. *Eur Respir J.* 2007; 30(4):623–626. [PubMed: 17690121]
14. Barry CE, Boshoff HI, Dartois V, Dick T, Ehrst S, Flynn J, Schnappinger D, Wilkinson RJ, Young D. The Spectrum of Latent Tuberculosis: Rethinking the Biology and Intervention Strategies. *Nat Rev Microbiol.* 2009; 7:845–855. [PubMed: 19855401]
15. Dye C. Global Burden of Tuberculosis: Estimated Incidence, Prevalence, and Mortality by Country. *JAMA J Am Med Assoc.* 1999; 282(7):677.
16. Zumla A, Nahid P, Cole ST. Advances in the Development of New Tuberculosis Drugs and Treatment Regimens. *Nat Rev Drug Discovery.* 2013; 12(5):388–404. [PubMed: 23629506]
17. Mdluli K, Kaneko T, Upton A. The Tuberculosis Drug Discovery and Development Pipeline and Emerging Drug Targets. *Cold Spring Harbor Perspect Med.* 2015; 5(6):a021154–a021154.
18. Cole ST, Riccardi G. New Tuberculosis Drugs on the Horizon. *Curr Opin Microbiol.* 2011; 14(5): 570–576. [PubMed: 21821466]
19. Evangelopoulos D, McHugh TD. Improving the Tuberculosis Drug Development Pipeline. *Chem Biol Drug Des.* 2015; 86(5):951–960. [PubMed: 25772393]
20. Koul A, Arnoult E, Lounis N, Guillemont J, Andries K. The Challenge of New Drug Discovery for Tuberculosis. *Nature.* 2011; 469(7331):483–490. [PubMed: 21270886]
21. Salaemae W, Azhar A, Booker GW, Polyak SW. Biotin Biosynthesis in Mycobacterium Tuberculosis: Physiology, Biochemistry and Molecular Intervention. *Protein Cell.* 2011; 2(9):691–695. [PubMed: 21976058]

22. Marquet A, Bui BT, Florentin D. Biosynthesis of Biotin and Lipoic Acid. *Vitam Horm* (London, UK). 2001; 61:51–101.
23. Said HM. Cell and Molecular Aspects of Human Intestinal Biotin Absorption. *J Nutr*. 2008; 139(1):158–162. [PubMed: 19056639]
24. Cronan JE, Lin S. Synthesis of the A, ω -Dicarboxylic Acid Precursor of Biotin by the Canonical Fatty Acid Biosynthetic Pathway. *Curr Opin Chem Biol*. 2011; 15(3):407–413. [PubMed: 21435937]
25. Stoner GL, Eisenberg MA. Purification and Properties of 7, 8-Diaminopelargonic Acid Aminotransferase. *J Biol Chem*. 1975; 250(11):4029–4036. [PubMed: 1092681]
26. Stoner GL, Eisenberg MA. Biosynthesis of 7, 8-Diaminopelargonic Acid from 7-Keto-8-Aminopelargonic Acid and S-Adenosyl-L-Methionine. The Kinetics of the Reaction. *J Biol Chem*. 1975; 250(11):4037–4043. [PubMed: 1092682]
27. Mann S, Ploux O. 7,8-Diaminopelargonic Acid Aminotransferase from *Mycobacterium Tuberculosis*, a Potential Therapeutic Target: Characterization and Inhibition Studies. *FEBS J*. 2006; 273(20):4778–4789. [PubMed: 16984394]
28. Park SW, Klotzsche M, Wilson DJ, Boshoff HI, Eoh H, Manjunatha U, Blumenthal A, Rhee K, Barry CE, Aldrich CC, Ehrt S, Schnappinger D. Evaluating the Sensitivity of *Mycobacterium Tuberculosis* to Biotin Deprivation Using Regulated Gene Expression. *PLoS Pathog*. 2011; 7(9):e1002264. [PubMed: 21980288]
29. Dey S, Lane JM, Lee RE, Rubin EJ, Sacchettini JC. Structural Characterization of the *Mycobacterium Tuberculosis* Biotin Biosynthesis Enzymes 7,8-Diaminopelargonic Acid Synthase and Dethiobiotin Synthetase. *Biochemistry*. 2010; 49(31):6746–6760. [PubMed: 20565114]
30. Dai R, Wilson DJ, Geders TW, Aldrich CC, Finzel BC. Inhibition of *Mycobacterium Tuberculosis* Transaminase BioA by Aryl Hydrazines and Hydrazides. *ChemBioChem*. 2014; 15(4):575–586. [PubMed: 24482078]
31. Shi C, Geders TW, Park SW, Wilson DJ, Boshoff HI, Abayomi O, Barry CE, Schnappinger D, Finzel BC, Aldrich CC. Mechanism-Based Inactivation by Aromatization of the Transaminase BioA Involved in Biotin Biosynthesis in *Mycobacterium Tuberculosis*. *J Am Chem Soc*. 2011; 133(45):18194–18201. [PubMed: 21988601]
32. Kitahara T, Hotta K, Yoshida M, Okami Y. Biological Studies on Amiclenomycin. *J Antibiot*. 1975; 28(3):215–221. [PubMed: 805118]
33. Okami Y, Kitahara T, Hamada M, Naganawa H, Kondo S, Maeda K, Takeuchi T, Umezawa H. Studies on a New Amino Acid Antibiotic, Amiclenomycin. *J Antibiot*. 1974; 27(9):656–664. [PubMed: 4436150]
34. Wilson DJ, Shi C, Duckworth BP, Muretta JM, Manjunatha U, Sham YY, Thomas DD, Aldrich CC. A Continuous Fluorescence Displacement Assay for BioA: An Enzyme Involved in Biotin Biosynthesis. *Anal Biochem*. 2011; 416(1):27–38. [PubMed: 21621502]
35. Park SW, Casalena DE, Wilson DJ, Dai R, Nag PP, Liu F, Boyce JP, Bittker JA, Schreiber SL, Finzel BC, Schnappinger D, Aldrich CC. Target-Based Identification of Whole-Cell Active Inhibitors of Biotin Biosynthesis in *Mycobacterium Tuberculosis*. *Chem Biol* (Oxford, UK). 2015; 22(1):76–86.
36. Dai, R. Fragment Based Inhibitor Design of *Mycobacterium Tuberculosis* BioA Dissertation. University of Minnesota; Minneapolis, MN: 2015.
37. Costantino L, Barlocco D. Privileged Structures as Leads in Medicinal Chemistry. *Curr Med Chem*. 2006; 13(1):65–85. [PubMed: 16457640]
38. Dai R, Geders TW, Liu F, Park SW, Schnappinger D, Aldrich CC, Finzel BC. Fragment-Based Exploration of Binding Site Flexibility in *Mycobacterium Tuberculosis* BioA. *J Med Chem*. 2015; 58(13):5208–5217. [PubMed: 26068403]
39. Chaires JB. Calorimetry and Thermodynamics in Drug Design. *Annu Rev Biophys*. 2008; 37(1): 135–151. [PubMed: 18573076]
40. Freire E. Do Enthalpy and Entropy Distinguish First in Class from Best in Class? *Drug Discovery Today*. 2008; 13(19–20):869–874. [PubMed: 18703160]
41. Ruben AJ, Kiso Y, Freire E. Overcoming Roadblocks in Lead Optimization: A Thermodynamic Perspective. *Chem Biol Drug Des*. 2006; 67(1):2–4. [PubMed: 16492143]

42. Wang T, Zhang Z, Meanwell NA. Benzoylation of Dianions: Preparation of Monobenzoylated Derivatives of Symmetrical Secondary Diamines. *J Org Chem.* 1999; 64(20):7661–7662.
43. Wolfe JP, Wagaw S, Buchwald SL. An Improved Catalyst System for Aromatic Carbon–Nitrogen Bond Formation: The Possible Involvement of Bis(Phosphine) Palladium Complexes as Key Intermediates. *J Am Chem Soc.* 1996; 118(30):7215–7216.
44. Chakraborty A, Dey S, Sawoo S, Adarsh NN, Sarkar A. Regioselective 1,3-Dipolar Cycloaddition Reaction of Azides with Alkoxy Alkynyl Fischer Carbene Complexes. *Organometallics.* 2010; 29(23):6619–6622.
45. Li J, Zhang X, Zhang Z, Padakanti PK, Jin H, Cui J, Li A, Zeng D, Rath NP, Flores H, Perlmutter JS, Parsons SM, Tu Z. Heteroaromatic and Aniline Derivatives of Piperidines As Potent Ligands for Vesicular Acetylcholine Transporter. *J Med Chem.* 2013; 56(15):6216–6233. [PubMed: 23802889]
46. Geders TW, Gustafson K, Finzel BC. Use of Differential Scanning Fluorimetry to Optimize the Purification and Crystallization of PLP-Dependent Enzymes. *Acta Crystallogr, Sect F: Struct Biol Cryst Commun.* 2012; 68(5):596–600.
47. Vonrhein C, Flensburg C, Keller P, Sharff A, Smart O, Paciorek W, Womack T, Bricogne G. Data Processing and Analysis with the *autoPROC* Toolbox. *Acta Crystallogr, Sect D: Biol Crystallogr.* 2011; 67(4):293–302. [PubMed: 21460447]
48. Kabsch W. *Acta Crystallogr, Sect D: Biol Crystallogr.* 2010; 66(2):125–132. [PubMed: 20124692]
49. McCoy AJ, Grosse-Kunstleve RW, Adams PD, Winn MD, Storoni LC, Read RJ. Phaser Crystallographic Software. *J Appl Crystallogr.* 2007; 40(4):658–674. [PubMed: 19461840]
50. Adams PD, Afonine PV, Bunkoczi G, Chen VB, Davis IW, Echols N, Headd JJ, Hung L-W, Kapral GJ, Grosse-Kunstleve RW, McCoy AJ, Moriarty NW, Oeffner R, Read RJ, Richardson DC, Richardson JS, Terwilliger TC, Zwart PH. PHENIX: A Comprehensive Python-Based System for Macromolecular Structure Solution. *Acta Crystallogr, Sect D: Biol Crystallogr.* 2010; 66(2):213–221. [PubMed: 20124702]
51. Afonine PV, Grosse-Kunstleve RW, Echols N, Headd JJ, Moriarty NW, Mustyakimov M, Terwilliger TC, Urzhumtsev A, Zwart PH, Adams PD. Towards Automated Crystallographic Structure Refinement with Phenix.refine. *Acta Crystallogr, Sect D: Biol Crystallogr.* 2012; 68(4):352–367. [PubMed: 22505256]
52. Emsley P, Cowtan K. Coot: Model-Building Tools for Molecular Graphics. *Acta Crystallogr, Sect D: Biol Crystallogr.* 2004; 60(12):2126–2132. [PubMed: 15572765]
53. Lebedev AA, Young P, Isupov MN, Moroz OV, Vagin AA, Murshudov GN. *JLigand*: A Graphical Tool for the *CCP4* Template-Restraint Library. *Acta Crystallogr, Sect D: Biol Crystallogr.* 2012; 68(4):431–440. [PubMed: 22505263]

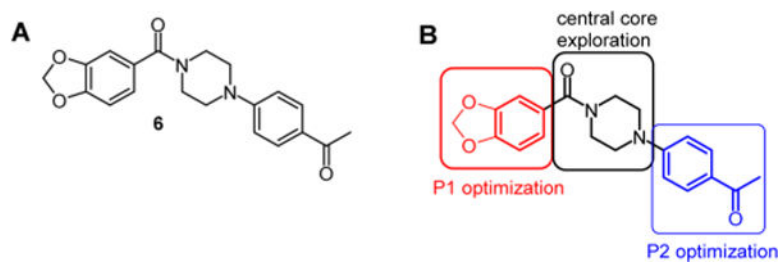


Figure 1.
(A) Structure of initial hit *N*-aryl, *N'*-benzoylpiperazine **6**. (B) Summary of SAR analysis.

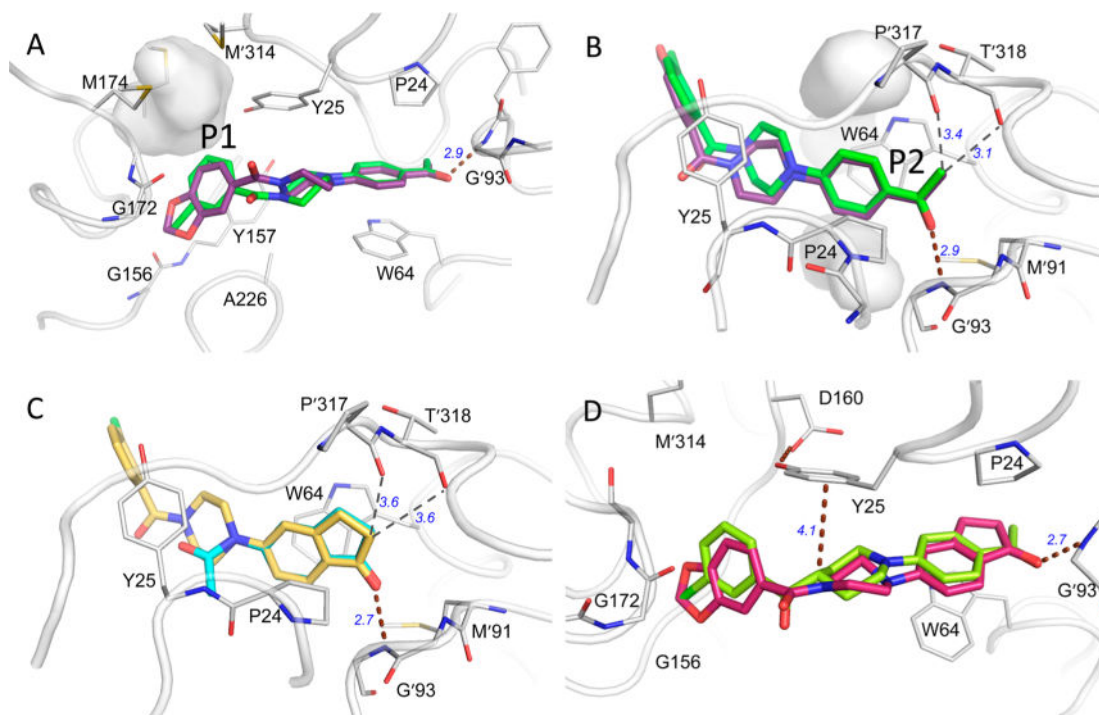


Figure 2.

(A) Comparison of **6** (purple, PDB ID: 4XJP) and **12** (green, PDB ID: 4W1X) in the binding pocket with residues that make substantial contact with the ligands. H-bonds are shown with brown dashed lines. Weaker nonbonded close contacts are illustrated with thin dashed lines. (A) The P1 subsite: the gray surface surrounds a cavity between Met165, Met 174, and Met '314 left unoccupied by ligand or protein atoms following ligand binding. (B) The P2 subsite: unoccupied cavities are also found both above and below the acetylphenyl ring in complexes with **6** and **12**. (C) Position of inden-1-one-containing fragment³⁸ (cyan, PDB ID: 4WYF) compared to that of compound **26** (yellow, PDB ID: 4XJO) in the same orientation as panel B. (D) Crystal structures with compounds **36** (red, PDB ID: 5KGS) and **39** (lime, PDB ID: 4KGT).

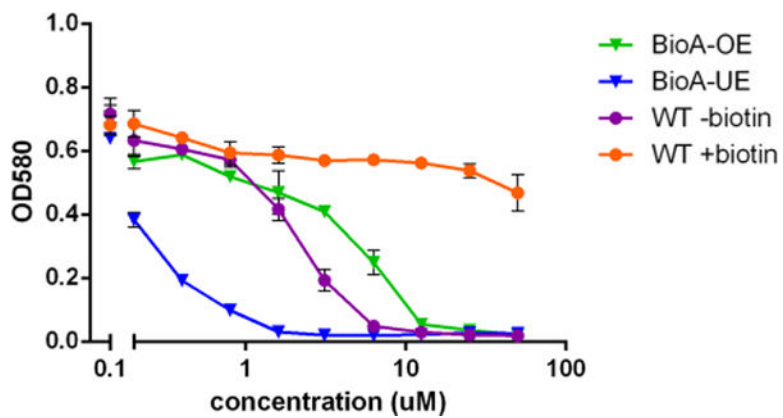


Figure 3. Inhibition of *Mtb* growth by compound **36**. A representative concentration–response plot for **36** showing *Mtb* growth on the *y*-axis as measured by the optical density at 580 nm versus the \log_{10} of the compound concentration on the *x*-axis. WT *Mtb* in biotin-free medium (purple), WT *Mtb* in biotin-containing medium (orange), Bio-UE (blue), and Bio-OE (green) *Mtb* strains in biotin-free medium.

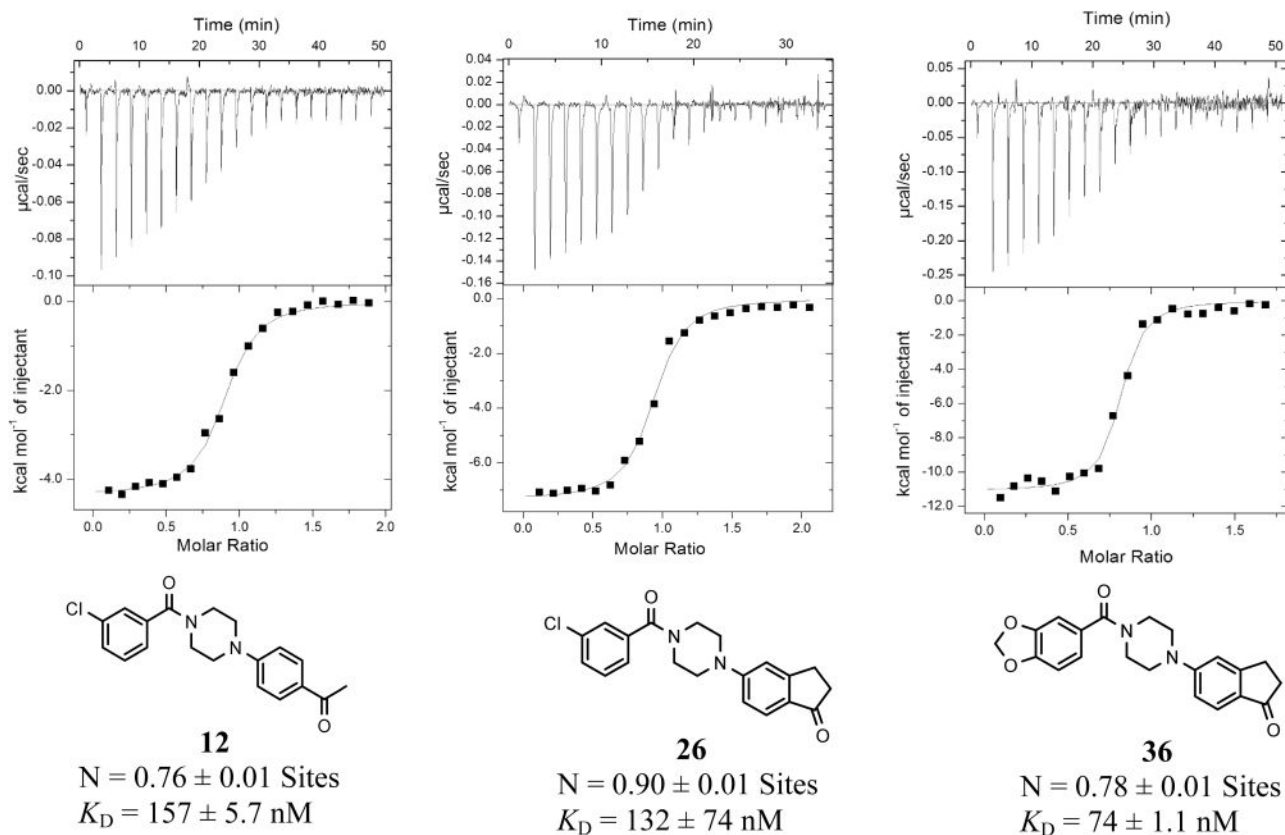
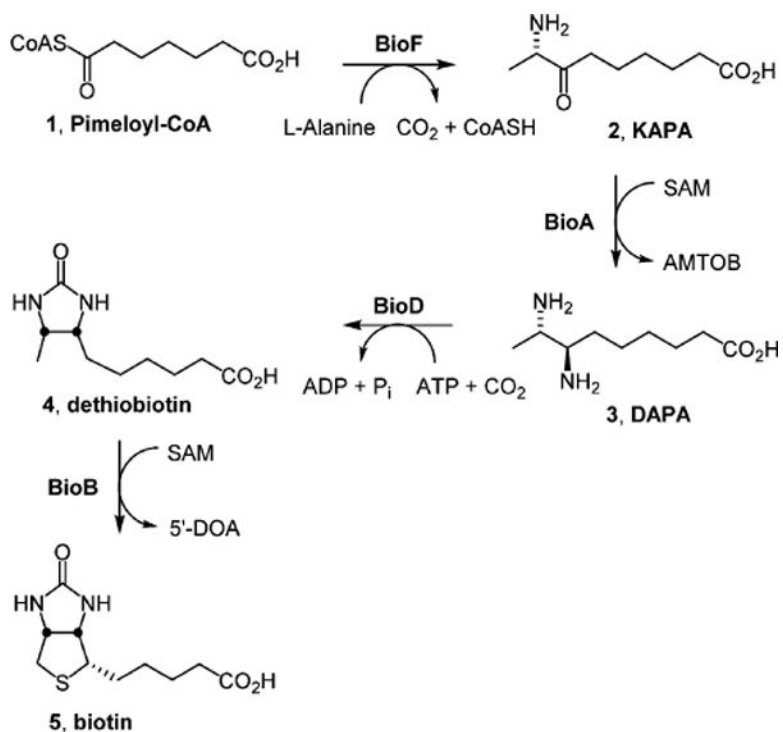
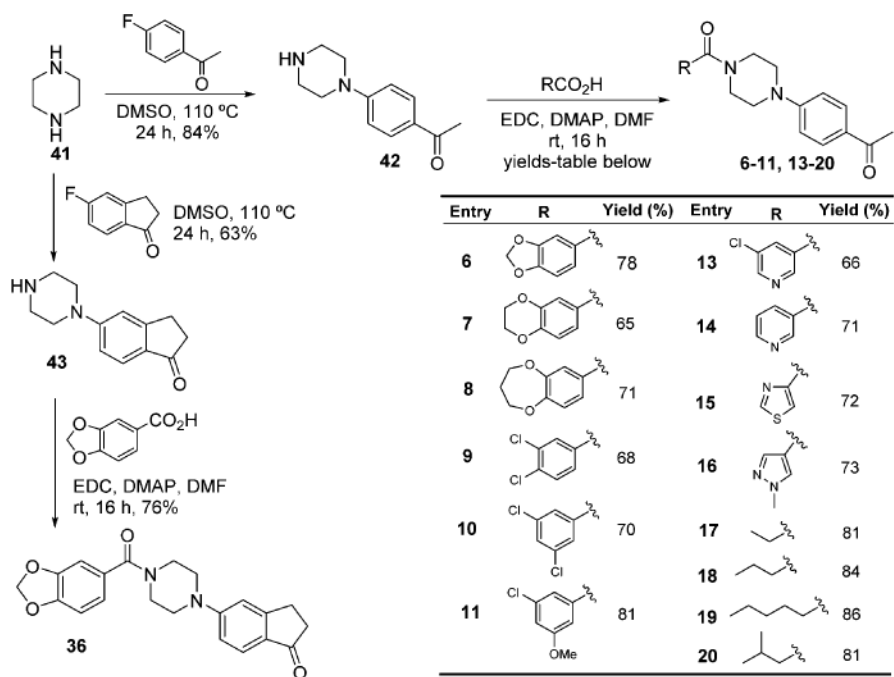


Figure 4. Representative ITC binding isotherms (top) and integrated enthalpy curves (bottom) for **12**, **26**, and **36** ($100 \mu\text{M}$) with BioA ($10 \mu\text{M}$).

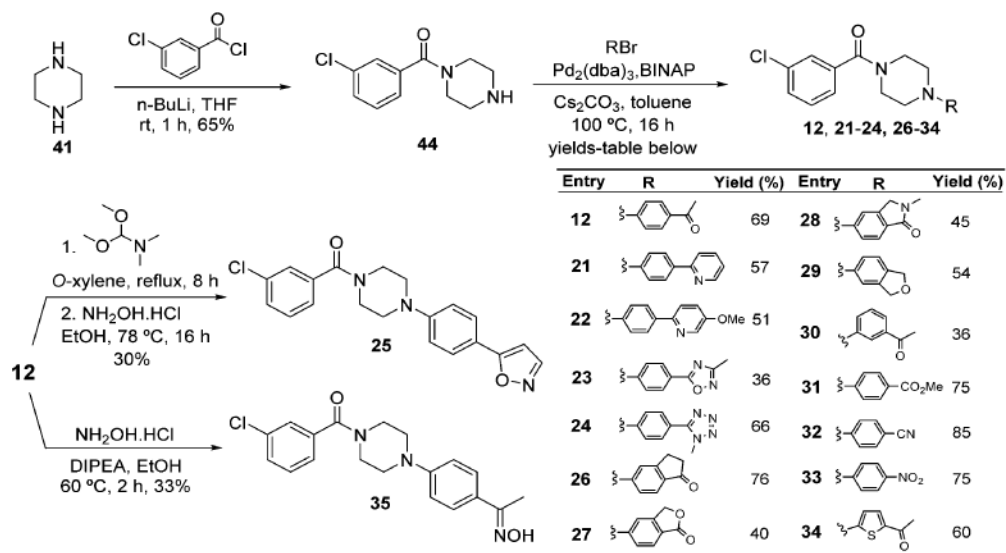


Scheme 1. Late Steps of the Biotin Biosynthesis Pathway in *Mtb*^a

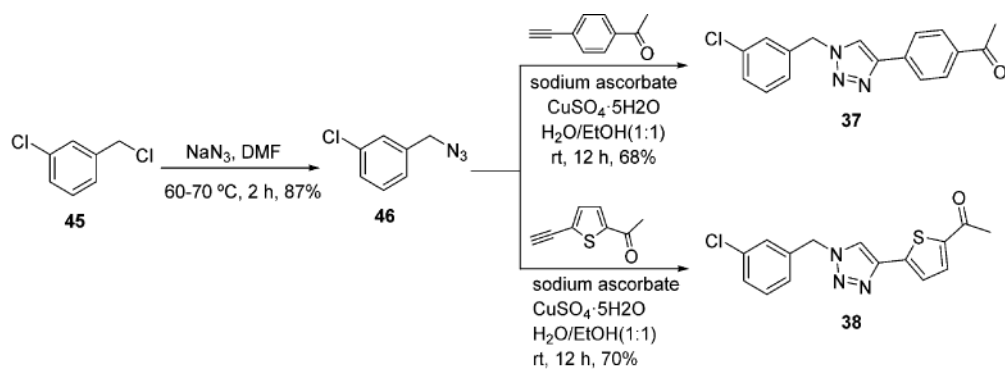
^aBioF catalyzes the decarboxylative condensation of pimeloyl-CoA **1** with alanine to furnish 8-aminopelargonic acid (KAPA, **2**). The PLP-dependent aminotransferase BioA performs the reductive amination of KAPA **2** to 7,8-diaminopelargonic acid (DAPA, **3**). BioD-mediated carboxylation of DAPA **3** provides dethiobiotin **4**, which is converted to biotin **5** by the radical SAM enzyme BioB.



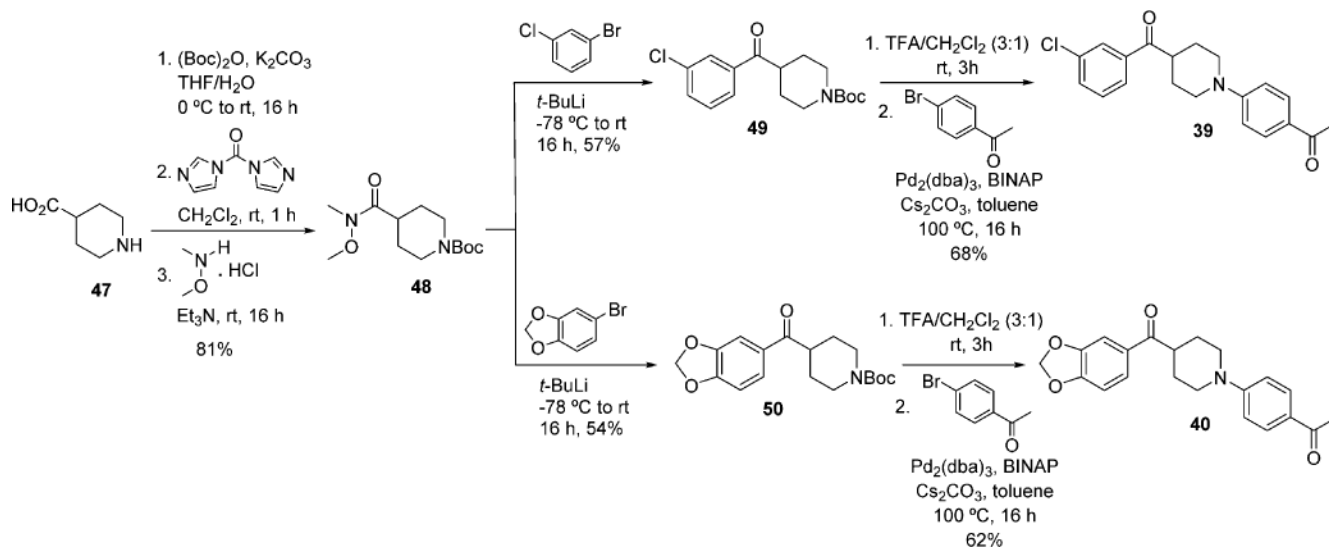
Scheme 2.
Modification of the Benzodioxolyl Ring



Scheme 3.
Modification of the Acetophenyl Ring





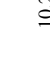

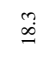
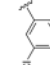
Scheme 4.
Modification of Linker with 1,2,3-Triazoles



Scheme 5.
Modification of Linker with Piperidine

Table 1

SAR of the Methylene-3,4-dioxybenzoyl Moiety

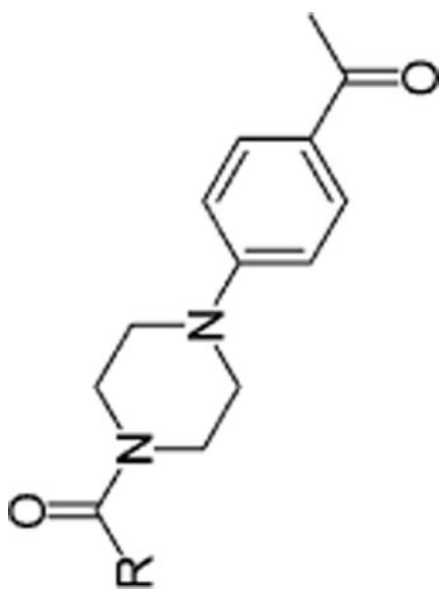
Compound	R	MIC ₅₀ (μM)			
		BioA-UE ^a	BioA-OE ^b	WT-biotin ^c	WT+biotin ^d
6		0.4 (1.7) ^e	31.1 (>50) ^e	5.6 (23.4) ^e	>50 (>50) ^e
7		10.4	>50	>50	>50
8		21.1	>50	>50	>50
9		1.9	17.7	10.2	10.7
10		>50	>50	>50	>50
11		18.3	>50	28.6	39.1

Author Manuscript

Author Manuscript

Author Manuscript

Author Manuscript



Compound	R	MIC ₅₀ (μM)				
		BioA-UE ^a	BioA-OE ^b	WT-biotin ^c	WT+biotin ^d	
12		0.5	7.5	5.1	30.1	
13		>50	>50	>50	>50	
14		14.6	>50	>50	>50	
15		>50	>50	>50	>50	
16		11.3	>50	>50	>50	
17		>50	>50	>50	>50	
18		>50	>50	>50	>50	
19		10.6	47.6	8.7	6.2	
20		>50	>50	>50	>50	

^aMinimum inhibitory concentration (MIC) that results in 50% inhibition against the *Mtb* BioA underexpression strain.

^bMIC that results in 50% inhibition against the *Mtb* BioA overexpression strain.

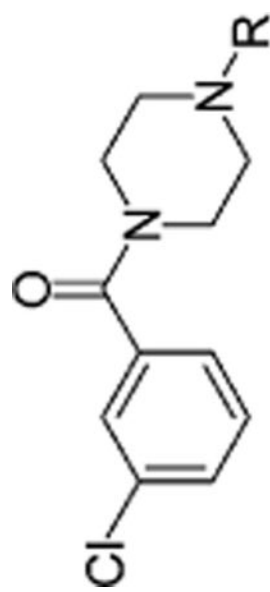
^cMIC that results in 50% inhibition against *Mtb* H37Rv without supplemental biotin.



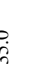
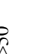



^dMIC that results in 50% inhibition against *Mtb* H37Rv with 1 μ M supplemental biotin.

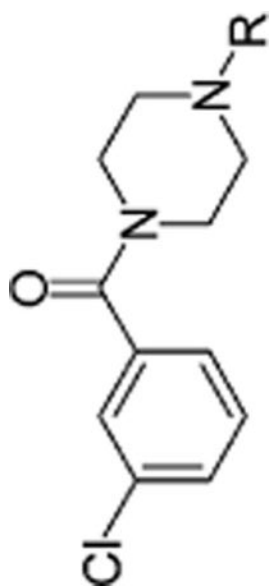
^eMIC that results in 90% inhibition.

Table 2

SAR of the Acetylphenyl Moiety



Compound	R	MIC ₅₀ (μM)			
		BioA-UE	BioA-OE	WT-biotin	WT+biotin
12		0.5	7.5	5.1	30.1
21		>50	>50	>50	>50
22		24.4	>50	22.0	>50
23		>50	>50	>50	>50
24		>50	>50	>50	>50
25		0.4	38.9	6.7	>50
26		0.3	8.1	4.4	47.0
27		1.8	>50	35.0	>50
28		1.2	>50	15.2	>50



Compound	R	MIC ₅₀ (μM)			
		BioA-UE	BioA-OE	WT-biotin	WT+biotin
29		12.8	>50	40.8	48.0
30		26.6	>50	>50	47.1
31		>50	>50	>50	>50
32		44.8	45.9	18.5	22.7
33		4.7	20.9	15.4	11.8
34		1.1	7.6	9.9	19.0
35		15.1	>50	20.4	39.1

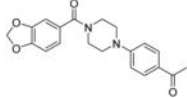
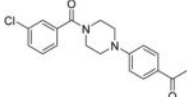
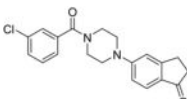
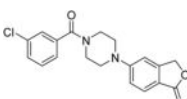
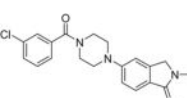
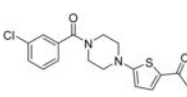
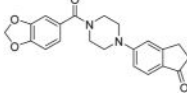
Table 3

SAR of the Piperazine Linker

Compound	Structure	MIC ₅₀ (μM)			
		BioA-UE	BioA-OE	WT-biotin	WT+biotin
6		0.4	31.1	5.6	>50
12		0.5	7.5	5.1	30.1
36		0.3	2.8	1.7	>50
37		24.4	>50	22.0	>50
38		>50	>50	>50	>50
39		6.8	9.2	4.1	3.3
40		>50	>50	>50	>50

Table 4

ITC Data of Selected Compounds

Compound	Structure	K_D (nM)	H (kcal/mol)	$-T \Delta S$ (kcal/mol)
6 ³⁵		108 ± 1	-11.8	2.3
12		157 ± 6	-4.4	-4.9
26		132 ± 74	-7.3	-2.1
27		685 ± 14	-3.2	-5.2
28		866 ± 19	-3.5	-4.7
34		322 ± 3	-7.0	-1.8
36		74 ± 1	-11.1	1.4